Cell Metabolism

Article

Central glucagon-like peptide 1 receptor activation inhibits Toll-like receptor agonist-induced inflammation

Graphical abstract

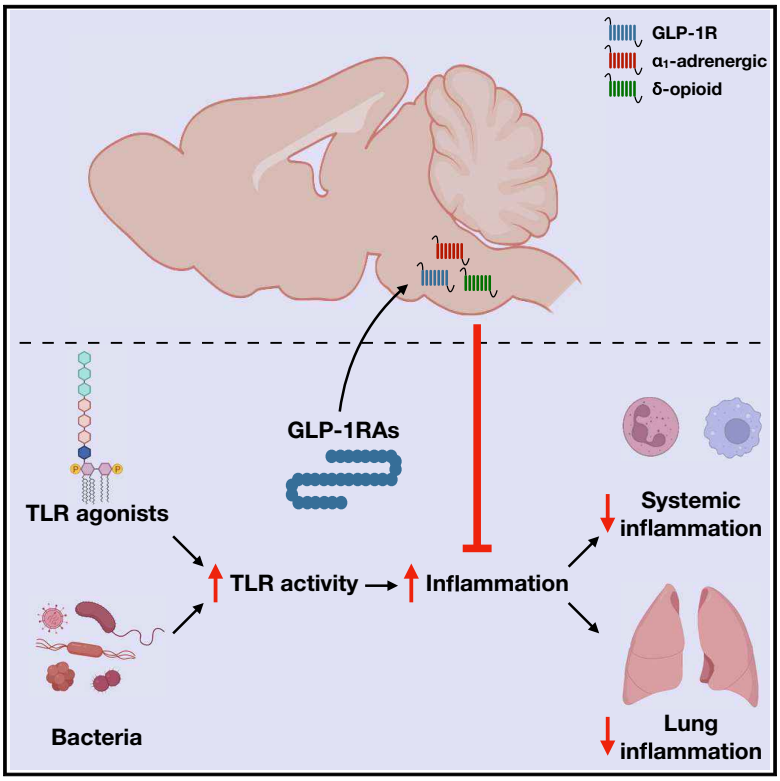

Authors

Chi Kin Wong, Brent A. McLean, Laurie L. Baggio, ..., Randy J. Seeley, Theodore J. Brown, Daniel J. Drucker

Correspondence

drucker@lunenfeld.ca

In brief

GLP-1R agonists may reduce cardiometabolic complications in part through reduction of inflammation. Here we show, using pharmacology and genetics, that the anti-inflammatory actions of GLP-1RAs to reduce TLR-mediated inflammation require CNS GLP-1R signaling.

Highlights

- GLP-1R agonism attenuates TLR-induced inflammation
- Semaglutide reduces the severity of polymicrobial inflammation
- Anti-inflammatory actions of GLP-1R agonists require CNS GLP-1Rs
- GLP-1R agonists reduce inflammation through CNS adrenergic and opioid GPCRs

Wong et al., 2024, Cell Metabolism *36*, 1–14
January 2, 2024
https://doi.org/10.1016/j.cmet.2023.11.009

CellPress

Cell Metabolism

CellPress

Article

Central glucagon-like peptide 1 receptor activation inhibits Toll-like receptor agonist-induced inflammation

Chi Kin Wong,[1] Brent A. McLean,[1] Laurie L. Baggio,[1] Jacqueline A. Koehler,[1] Rola Hammoud,[1] Nikolaj Rittig,[2,3] Julian M. Yabut,[1] Randy J. Seeley,[4] Theodore J. Brown,[1,5] and Daniel J. Drucker[1,6,7,*]

[1]Lunenfeld-Tanenbaum Research Institute, Sinai Health System, Toronto, ON, Canada
[2]Medical/Steno Aarhus Research Laboratory, Aarhus University Hospital, Aarhus University, Aarhus, Denmark
[3]Steno Diabetes Center Aarhus, Aarhus University Hospital, Aarhus, Denmark
[4]Department of Surgery, University of Michigan, Ann Arbor, MI, USA
[5]Department of Obstetrics and Gynecology, University of Toronto, Toronto, ON, Canada
[6]Department of Medicine, University of Toronto, Toronto, ON, Canada
[7]Lead contact
*Correspondence: drucker@lunenfeld.ca
https://doi.org/10.1016/j.cmet.2023.11.009

SUMMARY

Glucagon-like peptide-1 receptor agonists (GLP-1RAs) exert anti-inflammatory effects relevant to the chronic complications of type 2 diabetes. Although GLP-1RAs attenuate T cell-mediated gut and systemic inflammation directly through the gut intraepithelial lymphocyte GLP-1R, how GLP-1RAs inhibit systemic inflammation in the absence of widespread immune expression of the GLP-1R remains uncertain. Here, we show that GLP-1R activation attenuates the induction of plasma tumor necrosis factor alpha (TNF-α) by multiple Toll-like receptor agonists. These actions are not mediated by hematopoietic or endothelial GLP-1Rs but require central neuronal GLP-1Rs. In a cecal slurry model of polymicrobial sepsis, GLP-1RAs similarly require neuronal GLP-1Rs to attenuate detrimental responses associated with sepsis, including sickness, hypothermia, systemic inflammation, and lung injury. Mechanistically, GLP-1R activation leads to reduced TNF-α via α_1-adrenergic, δ-opioid, and κ-opioid receptor signaling. These data extend emerging concepts of brain-immune networks and posit a new gut-brain GLP-1R axis for suppression of peripheral inflammation.

INTRODUCTION

Glucagon-like peptide 1 receptor agonists (GLP-1RAs) are peptide-based medications used to lower blood glucose and body weight in people with type 2 diabetes (T2D) and obesity.[1] GLP-1RAs also reduce major adverse cardiovascular events in people with T2D and obesity[2] and are being explored in late-stage clinical trials for treatment of metabolic-associated fatty liver disease[3] and neurodegenerative diseases, including Parkinson's disease and Alzheimer's disease.[4] Although the anti-inflammatory efficacy of GLP-1RAs likely reflect reductions in glucose and body weight,[5] direct or indirect engagement of the GLP-1R with the immune system may also contribute.

GLP-1RAs reduce myeloid-cell-driven inflammation in mouse models with diet-induced obesity,[6] diet-induced steatohepatitis,[7–9] experimental atherosclerosis or nephritis,[8,10] coronary artery ligation-induced myocardial infarction,[11] and diet-induced cardiomyopathy.[12] Reconciling these anti-inflammatory benefits of GLP-1RAs with evidence for GLP-1R expression in immune cells is challenging because myeloid cells express low levels of the canonical GLP-1R,[5,13] and in several mouse models, GLP-1RAs retain their efficacy in mice lacking hematopoietic cell GLP-1Rs.[8,11] Although some anti-inflammatory effects of GLP-1RAs have been attributed to GLP-1R-expressing T cells,[8,14,15] the T cell GLP-1R alone was insufficient to explain the anti-inflammatory actions of GLP-1RAs on myeloid cells.[14] Hence, the GLP-1R-expressing cell type(s) responsible for the systemic anti-inflammatory actions ensuing from GLP-1R activation remain incompletely characterized.

Myeloid cells, particularly monocytes and macrophages, express a variety of Toll-like receptors (TLRs) that recognize bacterial and viral components.[16] The prototypical TLR4 agonist lipopolysaccharide (LPS) is an outer cell membrane component of gram-negative bacteria that potently activates myeloid cells.[16] Activation of TLR4 signaling stimulates production of tumor necrosis factor alpha (TNF-α), interleukin 1 beta (IL-1β), and interleukin 6 (IL-6), together with other pro-inflammatory cytokines.[16] This TLR4 response is conserved across other TLRs,[17] and these receptor pathways constitute a fundamental mechanism by which innate immune cells sense foreign pathogens and initiate inflammation.

Please cite this article in press as: Wong et al., Central glucagon-like peptide 1 receptor activation inhibits Toll-like receptor agonist-induced inflammation, Cell Metabolism (2023), https://doi.org/10.1016/j.cmet.2023.11.009

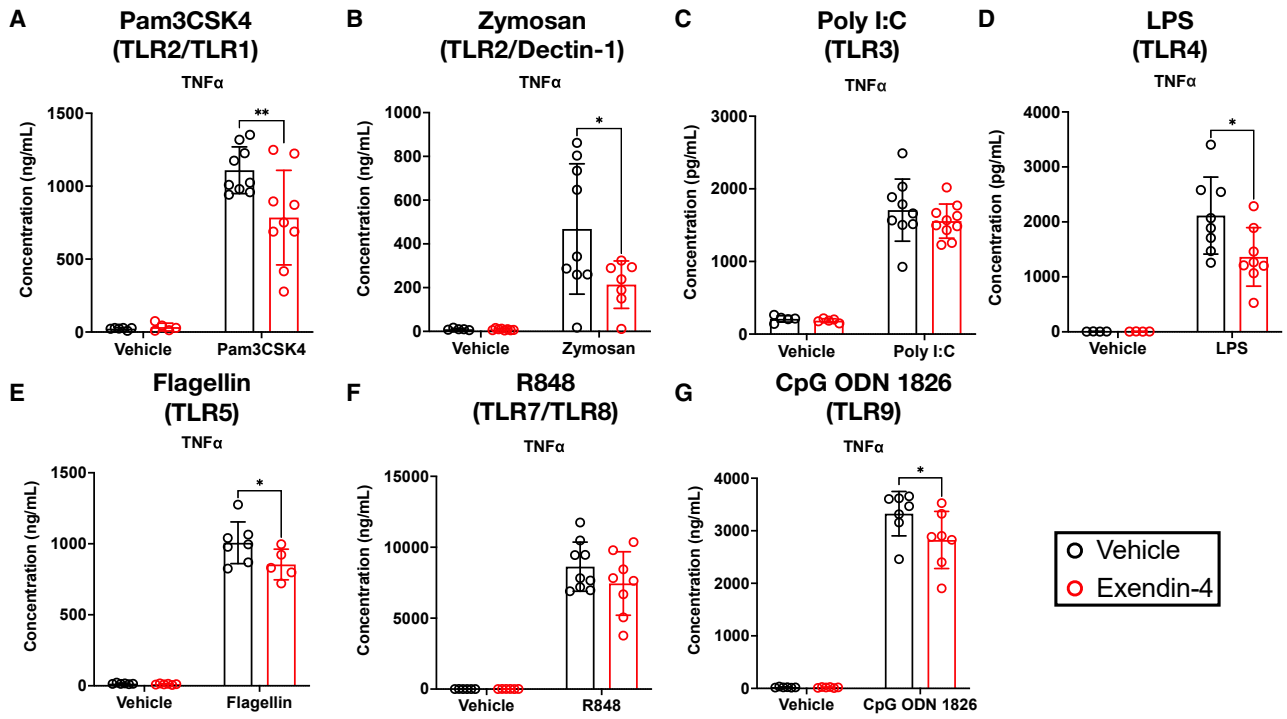

Figure 1. Exendin-4 prevents the full induction of plasma TNF-α by ligands of various Toll-like receptors

Plasma TNF-α levels in C57BL/6J mice treated with exendin-4 (10 nmol/kg) or vehicle (saline), together with the following Toll-like receptor agonists or vehicle (saline) i.p. (A) Pam3CSK4 (100 μg) for 1 h, (B) zymosan (300 μg) for 2 h, (C) poly I:C (100 μg) for 1 h, (D) lipopolysaccharides (35 μg) for 3 h, (E) flagellin (3 μg) for 1 h, (F) R848 (30 μg) for 1 h, or (G) CpG ODN 1826 (15 nmol) for 1 h. n = 4–10. Each panel was pooled from data of two independent experiments. Data are represented as mean ± SD. *p < 0.05, **p < 0.01. Two-way ANOVA tests with Sidak post hoc tests in (A), (B), (D), (E), and (G).

These innate immune responses are also controlled by the central nervous system (CNS), which regulates the peripheral immune system indirectly through both neural and hormonal signals.[18]

Both the endogenous GLP-1 system and exogenous GLP-1RAs regulate the peripheral immune response to LPS. GLP-1-producing enteroendocrine L cells express TLR4 and secrete GLP-1 upon exposure to LPS in an IL-6-dependent manner.[19] GLP-1RAs inhibit T cell-mediated inflammation via the gut T cell GLP-1R, but this receptor is dispensable for the inhibitory effects of GLP-1RAs on LPS-induced systemic inflammation.[14,20] Notably, these pathways are likely conserved across species because LPS increases L cell GLP-1 secretion in humans[19] and GLP-1RAs reduce biomarkers of inflammation in human subjects.[21,22] It remains unclear whether GLP-1RAs suppress inflammation induced by TLR agonists other than LPS and on which GLP-1R-expressing cell population(s) GLP-1RAs act to suppress LPS-induced inflammation.

Given the low levels of GLP-1R expression in most immune and myeloid cell types,[5] we hypothesized that GLP-1RAs inhibit LPS-induced inflammation by activating non-myeloid cells, specifically, neuronal GLP-1Rs. We first screened multiple TLR agonists to probe the generalizability of the anti-inflammatory effects of GLP-1RAs. We next challenged mice lacking the GLP-1R in hematopoietic cells or in neurons, with LPS and simultaneous administration of GLP-1RAs. We further explored the effects of GLP-1RAs on inflammation and the associated responses in a cecal slurry model of polymicrobial sepsis. Pharmacological studies identified inhibitory actions of GLP-1RAs on LPS-induced TNF-α via multiple distinct neuroendocrine signaling pathways. A combination of mouse genetics and probing of CNS pathways using intracerebroventricular (i.c.v.) administration of ligands and antagonists revealed that engagement of central neuronal GLP-1Rs suppressed peripheral inflammation.

RESULTS

GLP-1R activation diminishes the induction of plasma TNF-α by TLR agonists

To examine the anti-inflammatory effects of GLP-1RAs pursuant to activation of different TLRs, we injected mice intraperitoneally (i.p.) with the GLP-1RA exendin-4, utilized clinically as exenatide, and the following TLR agonists: Pam3CSK4 (TLR2/TLR1), zymosan (TLR2/dectin-1), polyinosinic:polycytidylic acid (poly I:C; TLR3), LPS (TLR4), flagellin from *Salmonella typhimurium* (TLR5), R848 (TLR7/TLR8), or CpG ODN 1826 (TLR9), followed by quantification of plasma cytokines 1–3 h later. All TLR agonists acutely raised plasma levels of TNF-α (Figures 1A–1G), and most increased levels of IL-10, IL-6, C-X-C motif ligand 1 (CXCL1), and IL-1β (Figures S1A–S1G). T cell cytokines, including interferon-γ (IFN-γ), IL-2, IL-4, and IL-5, were not induced appreciably by any of these TLR agonists (not shown). Exendin-4 lowered plasma TNF-α levels induced by numerous TLR agonists, including Pam3CSK4, zymosan, LPS, flagellin, and CpG ODN 1826 (Figures 1A, 1B, 1D, 1E, and 1G). For most of the TLR agonists studied, exendin-4 had no consistent effects on the plasma levels of IL-10, IL-6, CXCL1, or IL-1β (Figures S1A–S1G). Because

Please cite this article in press as: Wong et al., Central glucagon-like peptide 1 receptor activation inhibits Toll-like receptor agonist-induced inflammation, Cell Metabolism (2023), https://doi.org/10.1016/j.cmet.2023.11.009

exendin-4 produced the strongest decrease (~35%) in TNF-α induced by LPS among all TLR agonists tested (Figure 1D), we focused subsequent experiments on LPS, a commonly used stimulator of the innate immune system, to interrogate the mechanisms by which GLP-1RAs suppress TLR-induced systemic inflammation.

GLP-1R activation downregulates blood leukocyte and lung *Tnf* expression during LPS-induced inflammation

TNF-α is a key pro-inflammatory cytokine potently induced upon TLR activation in myeloid lineages, including monocytes, macrophages, and neutrophils.[23,24] To identify the tissues contributing to the reduced circulating levels of TNF-α, we quantified *Tnf* mRNA and TNF-α protein levels in cells and tissues of LPS-challenged mice treated with or without exendin-4. These included blood leukocytes, spleen, and lungs, which are rich in myeloid cells,[25] and jejunum and liver, where GLP-1R$^+$ immune cells reside.[8,15] 3 h of LPS treatment upregulated *Tnf* mRNA in all of these tissues, but only the jejunum and lungs exhibited elevated TNF-α protein content (Figures S2A and S2B). Nonetheless, exendin-4 neither downregulated *Tnf* mRNA nor TNF-α content in any of these tissues (Figures S2A and S2B).

Because exendin-4 had no effect on tissue TNF-α levels as assessed at 3 h, we treated mice with LPS and exendin-4 and assessed TNF-α after 1 h, a time point at which plasma TNF-α approaches maximum levels.[26] LPS treatment potently raised plasma TNF-α and IL-10 levels (Figure 2A), and co-administration of exendin-4 decreased plasma TNF-α and increased plasma IL-10 in response to LPS (Figure 2A). Furthermore, exendin-4 downregulated *Tnf* mRNA in blood leukocytes and lungs but not in the spleen, jejunum, or liver of mice exposed to LPS for 1 h (Figure 2B). Moreover, exendin-4 did not alter TNF-α content in the spleen, jejunum, liver, or lungs of these mice (Figure S2C).

We next examined genes relevant to TNF-α production in the blood leukocytes and lungs of mice treated with LPS and exendin-4 for 1 h. In blood leukocytes, exendin-4 did not alter the expression of *Adam17*, which encodes the enzyme that cleaves and releases TNF-α from cell membranes, monocyte/macrophage markers *Adgre1* and *Ccr2*, and *Il1b* and *Ccl4*, a monocyte/macrophage-derived cytokine and chemokine, respectively (Figure 2C). Although exendin-4 downregulated both *Ccl2* and *Il6* in blood leukocytes (Figure 2C), it did not lower plasma monocyte chemoattractant protein-1 (MCP-1; encoded by *Ccl2*) or IL-6 levels (Figure S2D). Exendin-4 upregulated *Tlr4* in blood leukocytes of mice treated with vehicle but not with LPS (Figure 2C). Exendin-4 did not alter the expression of these genes in the lungs of LPS-treated mice (Figure S2E).

Lower levels of plasma TNF-α may reflect a reduced number of myeloid cells in the blood. Flow cytometry experiments showed that leukocyte counts, including lymphocytes, Ly6C$^+$ monocytes, and Ly6G$^+$ neutrophils, were decreased with LPS treatment (Figure S2F). However, exendin-4 did not further modify the proportion of these cells in LPS-treated mice (Figure S2F). We also examined the peritoneal cavity, a primary responder site to LPS when administered via i.p. injection.[27] Exendin-4 had no effect on TNF-α levels or the number of F4/80$^+$ cells in the peritoneal lavage fluid of LPS-treated mice (Figures S2G and S2H). Hence, among the tissues surveyed, lower plasma TNF-α in exendin-4-treated mice was associated with downregulated *Tnf* expression in circulating leukocytes and lungs.

GLP-1RAs attenuate LPS-induced inflammation via actions requiring central neuronal GLP-1Rs

Although exendin-4 downregulated *Tnf* expression in blood leukocytes, these cells expressed very low levels of *Glp1r* compared with other tissues examined (Figure S2I). Nevertheless, to explore the possible link between leukocyte GLP-1R expression and the effect of exendin-4 on circulating TNF-α, we studied Tie2-Cre;*Glp1r*$^{flox/flox}$ (*Glp1r*$^{Tie2-/-}$) mice, which lack *Glp1r* in all hematopoietic and endothelial cell lineages.[11] We measured plasma TNF-α levels in *Glp1r*$^{Tie2-/-}$ mice treated with LPS and exendin-4 for 1 h. Plasma TNF-α was reduced following exendin-4 administration in Tie2-Cre;*Glp1r*$^{+/+}$ (*Glp1r*$^{Tie2+/+}$) and *Glp1r*$^{Tie2-/-}$ mice (Figure 3A). To examine whether this was a direct effect on immune cells, we cultured whole blood and splenocytes isolated from C57BL/6J mice with LPS and exendin-4, or dexamethasone as a control, for 6 h. In both whole blood and splenocytes, LPS-stimulated TNF-α release, and dexamethasone, but not exendin-4, directly reduced TNF-α release (Figure 3B). Therefore, hematopoietic and endothelial GLP-1Rs are not required for GLP-1RAs to reduce levels of LPS-stimulated TNF-α.

In mice, the GLP-1R is abundantly expressed in the hypothalamus and brainstem,[28,29] with both regions identified as critical for central and peripheral coordination of immune responses during systemic inflammation.[18,30] In *Wnt1*-Cre2;*Glp1r*$^{flox/flox}$ (*Glp1r*$^{Wnt1-/-}$) mice, *Glp1r* expression is reduced in both the hypothalamus and brainstem.[29] To test whether neuronal GLP-1Rs are required for the GLP-1R-dependent reduction in TNF-α, we treated control and *Glp1r*$^{Wnt1-/-}$ mice with exendin-4 and LPS for 1 h. Peripheral administration of exendin-4 lowered plasma TNF-α in *Wnt1*-Cre2; *Glp1r*$^{+/+}$ (*Glp1r*$^{Wnt1+/+}$) but not in *Glp1r*$^{Wnt1-/-}$ mice (Figure 3C). By contrast, plasma IL-10 levels were higher in both *Glp1r*$^{Wnt1+/+}$ and *Glp1r*$^{Wnt1-/-}$ mice treated with exendin-4 (Figure S3A), suggesting divergent mechanistic regulation of IL-10 vs. TNF-α by exendin-4. Importantly, exendin-4 downregulated *Tnf* mRNA in blood leukocytes of control but not *Glp1r*$^{Wnt1-/-}$ mice (Figure S3B). To independently verify the importance of CNS GLP-1Rs for the systemic anti-inflammatory actions of GLP-1RAs in a second mouse model exhibiting reduced *Glp1r* expression in the CNS, we repeated the LPS experiments in Nestin-Cre;*Glp1r*$^{flox/flox}$ (*Glp1r*$^{Nes-/-}$) mice, which exhibited more complete knockdown of *Glp1r* in the CNS including the brainstem and hypothalamus, relative to *Glp1r*$^{Wnt1-/-}$ mice.[29,31] Consistent with findings in *Glp1r*$^{Wnt1-/-}$ mice, exendin-4 prevented the full induction of LPS-induced plasma TNF-α in control mice but not in *Glp1r*$^{Nes-/-}$ mice (Figure 3D).

Glp1r expression is downregulated in the enteric nervous system of *Glp1r*$^{Wnt1-/-}$ mice[29] and, to a lesser extent, in the distal gut of *Glp1r*$^{Nes-/-}$ mice (Figure S3C). To independently determine whether exendin-4 acts on the CNS to influence plasma TNF-α, we injected C57BL/6J mice i.c.v. with the GLP-1R antagonist exendin(9-39), followed by i.p. injection of LPS and exendin-4 for 1 h. We first determined the extent to which i.c.v. administered exendin(9-39) enters the circulation. We quantified plasma exendin(9-39) levels in mice given various doses of exendin(9-39)

Please cite this article in press as: Wong et al., Central glucagon-like peptide 1 receptor activation inhibits Toll-like receptor agonist-induced inflammation, Cell Metabolism (2023), https://doi.org/10.1016/j.cmet.2023.11.009

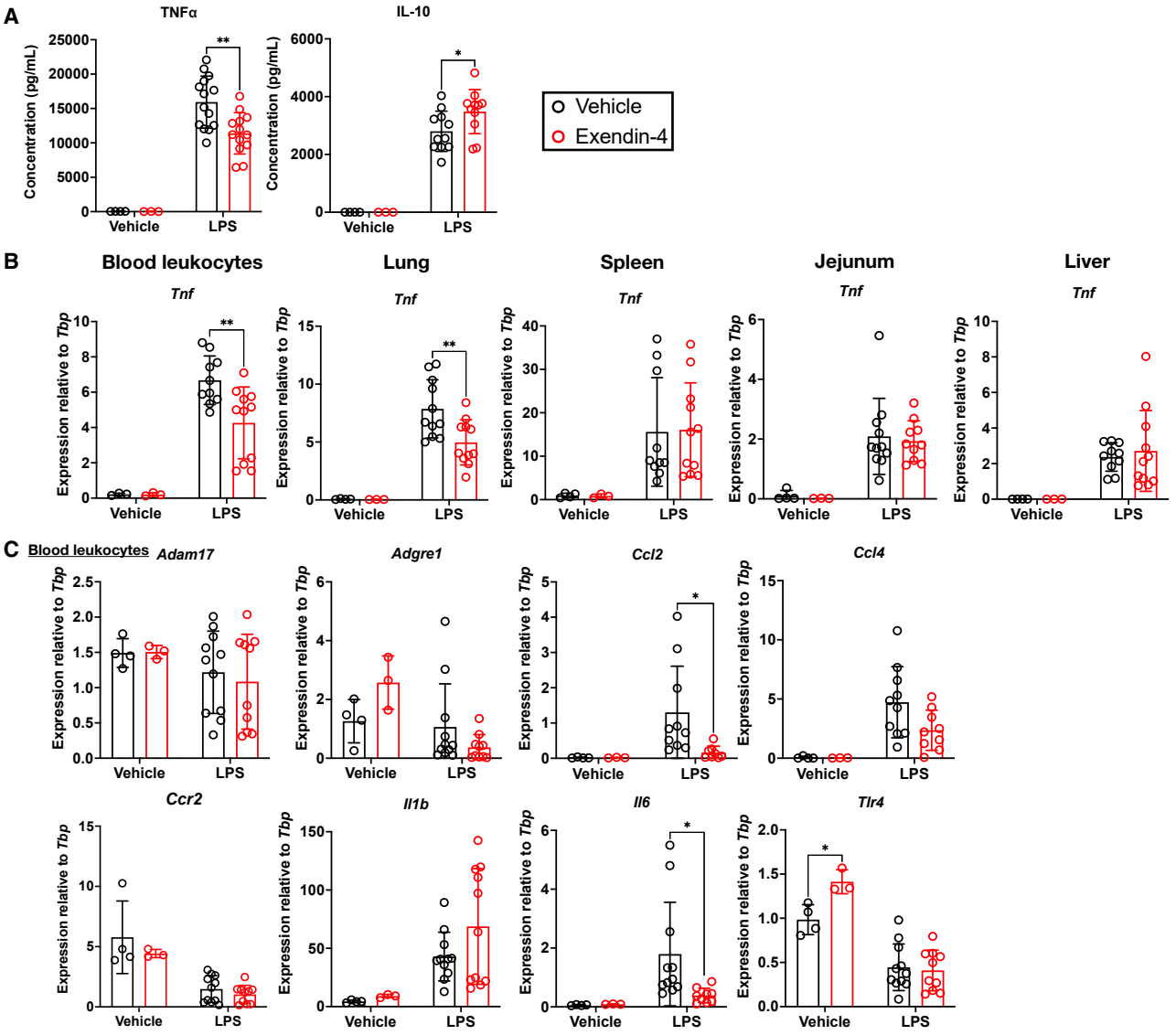

Figure 2. The decrease in LPS-induced TNF-α upon exendin-4 treatment is associated with downregulation of *Tnf* in blood leukocytes and lungs

(A) Plasma TNF-α and IL-10 in C57BL/6J mice treated with LPS (35 μg) or vehicle (saline) and exendin-4 (10 nmol/kg) or vehicle (saline) i.p. for 1 h. n = 3–14. Data were pooled from two independent experiments.

(B) Expression of *Tnf* in blood leukocytes, lungs, spleen, jejunum, and liver of C57BL/6J mice treated with LPS (35 μg) or vehicle (saline) and exendin-4 (10 nmol/kg) or vehicle (saline) i.p. for 1 h. Expression was reported relative to *Tbp* (a reference gene). n = 3–11. Data were pooled from two independent experiments.

(C) Expression of *Adam17*, *Adgre1*, *Ccl2*, *Ccl4*, *Ccr2*, *Il1b*, *Il6*, and *Tlr4* in blood leukocytes from C57BL/6J mice treated with LPS (35 μg) or vehicle (saline) and exendin-4 (10 nmol/kg) or vehicle (saline) i.p. for 1 h. Expression was reported relative to *Tbp* (a reference gene). n = 3–11. Data were pooled from two independent experiments.

Data are represented as mean ± SD. *p < 0.05, **p < 0.01. Two-way ANOVA tests with Sidak post hoc tests in (A)–(C).

i.c.v. or i.p. using an exendin-4 ELISA that recognizes the C terminus of exendin and thus cross-reacts with exendin(9-39) (Figure S3D). Exendin(9-39) given i.c.v. up to 1 μg did not raise plasma levels of immunoreactive exendin(9-39) (Figure 3E). However, a dose of 5 μg exendin(9-39) given i.c.v. raised plasma levels to 50% of the level seen in mice injected with 5 μg of exendin(9-39) i.p. (Figure 3E). Accordingly, we performed the i.c.v. experiments with 1 μg exendin(9-39). This dose of exendin(9-39) did not have a significant effect on LPS-induced TNF-α on its own, but it abolished the effect of systemically administered exendin-4 on plasma TNF-α (Figure 3F). Thus, a dose of exendin(9-39) given i.c.v. that was not detectable in the periphery eliminated the exendin-4-mediated decrease in plasma TNF-α.

To determine whether the anti-inflammatory actions of exendin-4 were evident with other structurally distinct GLP-1-based medications, we repeated the LPS experiments with semaglutide, a long-acting GLP-1RA, or tirzepatide, a GLP-1R and glucose-dependent insulinotropic peptide receptor (GIPR)

Please cite this article in press as: Wong et al., Central glucagon-like peptide 1 receptor activation inhibits Toll-like receptor agonist-induced inflammation, Cell Metabolism (2023), https://doi.org/10.1016/j.cmet.2023.11.009

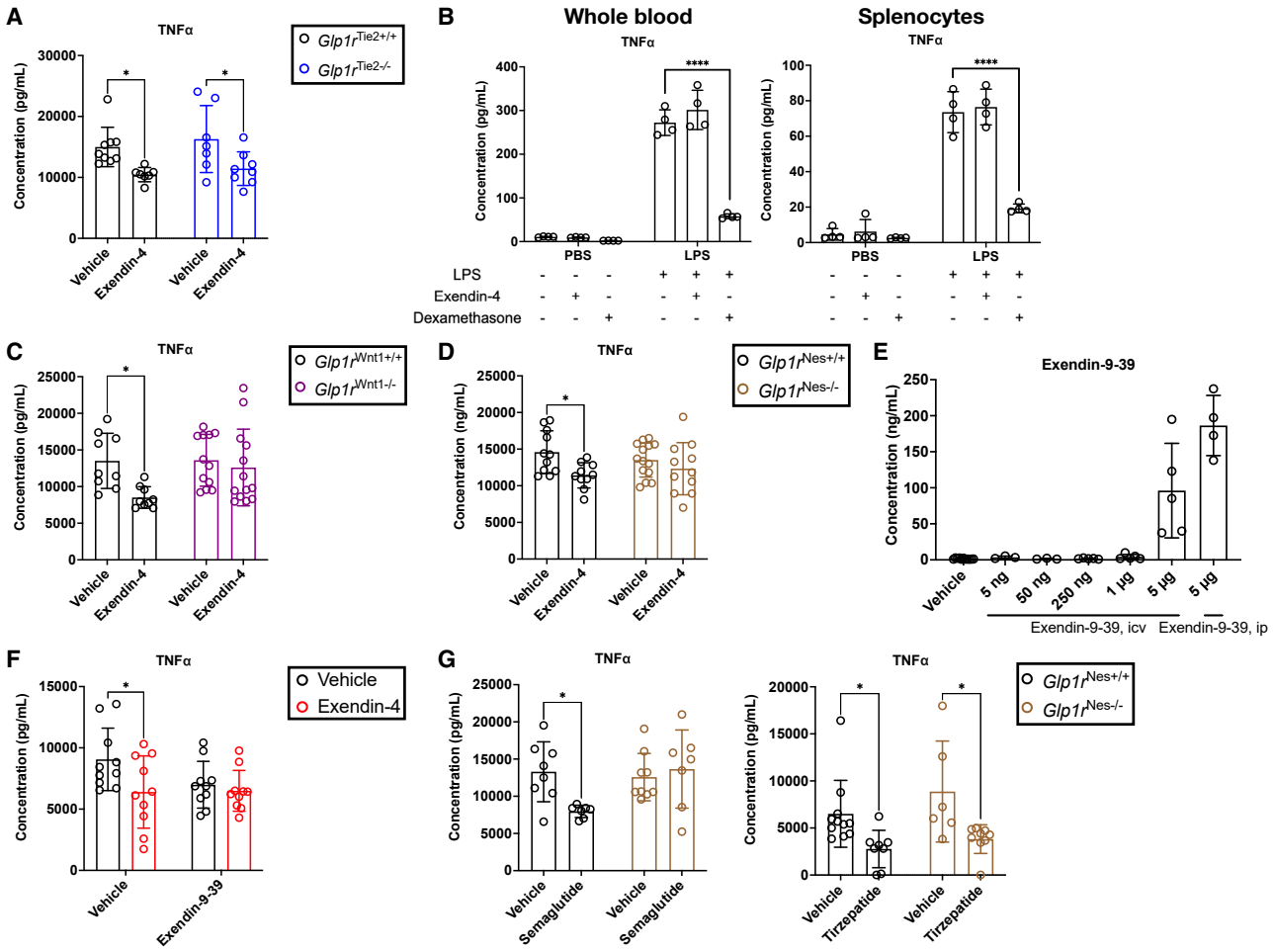

Figure 3. GLP-1RAs attenuate LPS-induced inflammation via actions requiring neuronal GLP-1Rs

(A) Plasma TNF-α levels in *Glp1r*$^{Tie2+/+}$ and *Glp1r*$^{Tie2-/-}$ mice treated with LPS (35 μg) and exendin-4 (10 nmol/kg) or vehicle (saline) i.p. for 1 h. n = 7–9. Data were pooled from two independent experiments.

(B) Supernatant TNF-α levels secreted by whole blood (left) and splenocytes (right) isolated from C57BL/6J mice and incubated with LPS (10 ng/mL), exendin-4 (50 nM), dexamethasone (1 μM), and/or vehicle (0.1% v/v ethanol) for 6 h. n = 4.

(C) Plasma TNF-α levels in *Glp1r*$^{Wnt1+/+}$ and *Glp1r*$^{Wnt1-/-}$ mice treated with LPS (35 μg) and exendin-4 (10 nmol/kg) or vehicle (saline) i.p. for 1 h. n = 9–13. Data were pooled from four independent experiments.

(D) Plasma TNF-α levels in *Glp1r*$^{Nes+/+}$ and *Glp1r*$^{Nes-/-}$ mice treated with LPS (35 μg) and exendin-4 (10 nmol/kg) or vehicle (saline) i.p. for 1 h. n = 10–14. Data were pooled from four independent experiments.

(E) Plasma exendin(9-39) levels in C57BL/6J mice injected with various doses of exendin(9-39) i.c.v. or i.p. or vehicle (saline) for 1.5 h. n = 3–11. Data were pooled from three independent experiments.

(F) Plasma TNF-α levels in C57BL/6J mice injected with exendin(9-39) (1 μg) i.c.v. for 30 min followed by LPS (35 μg) and exendin-4 (10 nmol/kg) or vehicle (saline) i.p. for 1 h. n = 10. Data were pooled from three independent experiments.

(G) Left: plasma TNF-α levels in *Glp1r*$^{Nes+/+}$ and *Glp1r*$^{Nes-/-}$ mice subcutaneously injected with semaglutide (2.44 nmol/kg) or vehicle (saline) for 1 h, followed by i.p. injection of LPS (35 μg) for 1 h. n = 7–9. Right: plasma TNF-α levels in *Glp1r*$^{Nes+/+}$ and *Glp1r*$^{Nes-/-}$ mice subcutaneously injected with tirzepatide (3 nmol/kg) or vehicle (saline) for 1 h, followed by i.p. injection of LPS (35 μg) for 1 h. n = 6–11. Data were pooled from two independent experiments.

Data are represented as mean ± SD. *p < 0.05, ****p < 0.0001. Two-way ANOVA tests with Sidak post hoc tests in (A)–(D), (F), and (G).

co-agonist,[32] in *Glp1r*$^{Nes-/-}$ mice. Semaglutide attenuated the induction of TNF-α by LPS in control but not in *Glp1r*$^{Nes-/-}$ mice (Figure 3G). In contrast, tirzepatide effectively prevented the full induction of TNF-α by LPS in both control and *Glp1r*$^{Nes-/-}$ mice (Figure 3G). Overall, our genetic and pharmacological experiments suggest that central neuronal GLP-1Rs are required for the systemic anti-inflammatory actions of peripherally administered GLP-1RAs.

GLP-1R activation attenuates sepsis-associated pathologies in a cecal slurry model of polymicrobial sepsis

Exendin-4 treatment attenuated the induction of plasma TNF-α by ligands of TLR1, TLR2, TLR4, TLR5, or TLR9 (Figure 1), receptors which recognize bacterial components.[17] Therefore, we hypothesized that neuronal GLP-1R activation similarly inhibits inflammation associated with bacterial infection. To test this

Please cite this article in press as: Wong et al., Central glucagon-like peptide 1 receptor activation inhibits Toll-like receptor agonist-induced inflammation, Cell Metabolism (2023), https://doi.org/10.1016/j.cmet.2023.11.009

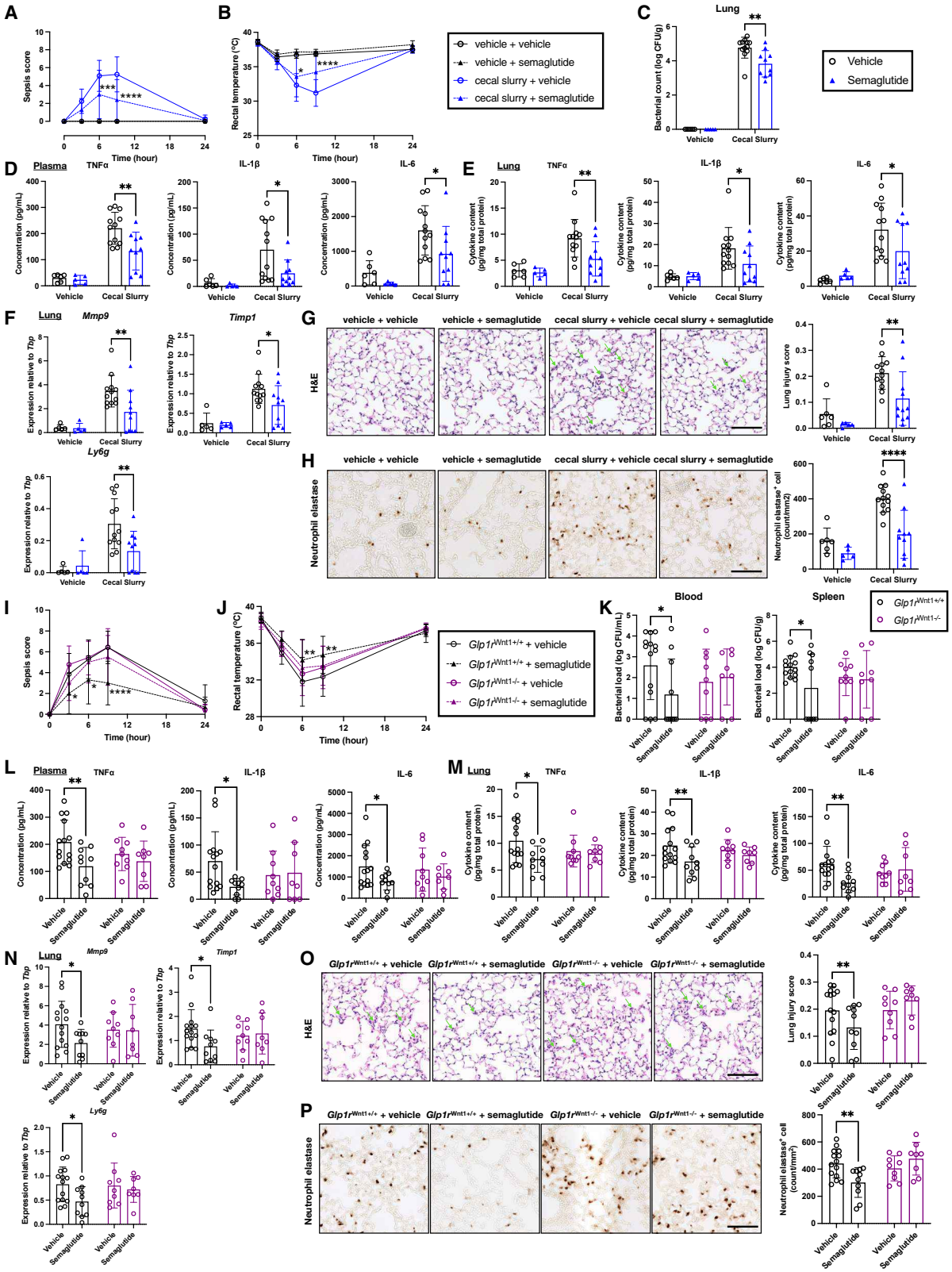

Figure 4. Semaglutide ameliorates multiple pathologies in a cecal slurry model of polymicrobial sepsis

(A and B) (A) Sepsis scores and (B) rectal temperature of C57BL/6J mice over 24 h after i.p. injection of vehicle or cecal slurry (600 μg/kg) and subcutaneous injection of vehicle or semaglutide (2.44 nmol/kg). n = 5–12. Data were pooled from two independent experiments.

(legend continued on next page)

Please cite this article in press as: Wong et al., Central glucagon-like peptide 1 receptor activation inhibits Toll-like receptor agonist-induced inflammation, Cell Metabolism (2023), https://doi.org/10.1016/j.cmet.2023.11.009

hypothesis, we injected mice with cecal slurry prepared from healthy C57BL/6J donors, a procedure that causes polymicrobial infection and induces myeloid-driven inflammation across multiple organs.[33] C57BL/6J mice injected with cecal slurry developed features of experimental sepsis within 24 h, including sepsis-associated sickness (Figure 4A), hypothermia (Figure 4B), and bacterial infection in multiple organs (Figures 4C and S4A). Concurrent treatment with semaglutide ameliorated the sickness and hypothermia in cecal slurry-exposed mice (Figures 4A and 4B). Semaglutide also decreased the bacterial load in the lungs (Figure 4C), but not in the blood, spleen, or liver (Figure S4A), of cecal slurry-treated mice. Similar to LPS, cecal slurry raised the circulating levels of multiple pro-inflammatory cytokines (Figures 4D and S4B). Notably, plasma levels of TNF-α, IL-1β, IL-6, and CXCL1 were lower in semaglutide-treated mice (Figures 4D and S4B). The semaglutide-treated mice had higher plasma IL-2 but not IFN-γ or IL-10 (Figure S4B).

Following observations that (1) lungs are particularly prone to injury caused by sepsis,[34] (2) liraglutide has been shown to protect against pathogen-associated inflammation in lungs,[35,36] and (3) exendin-4 downregulated *Tnf* in the lungs of LPS-treated mice (Figure 2B), we examined whether semaglutide attenuated sepsis-induced lung inflammation. Cecal slurry treatment increased lung TNF-α, IL-1β, IL-6, and CXCL1 content, whereas semaglutide decreased levels of these pro-inflammatory molecules in the lungs (Figures 4E and S4C). IL-2 was not detectable in the lungs of cecal slurry-treated mice. Neither cecal slurry nor semaglutide altered lung IFN-γ content; however, lung IL-10 content was lower in mice treated with cecal slurry and semaglutide (Figure S4C). Lung expression of *Tnf* and *Il1b*, but not *Il6*, was also lower in semaglutide-treated mice (Figure S4D).

Genes related to tissue remodeling and neutrophil infiltration, including *Mmp9*, *Timp1*, and *Ly6g*, were downregulated by semaglutide in the lungs of cecal slurry-treated mice (Figure 4F). Histological analyses revealed lung injury caused by cecal slurry injection featured neutrophil infiltration into the interstitium, mild septal thickening, collapsed alveoli, and interstitial hemorrhage (Figure 4G). The infiltration of neutrophils was independently confirmed by immunohistochemical analyses of neutrophil elastase (Figure 4H), a marker of activated neutrophils.[37] Consistent with the gene expression changes, the lung injury scores and the number of lung elastase-positive neutrophils were lower in the semaglutide group (Figures 4G and 4H).

We next performed the cecal slurry experiments in *Glp1r*$^{Wnt1-/-}$ mice. Cecal slurry-treated *Glp1r*$^{Wnt1-/-}$ mice exhibited sickness and hypothermia similar to control *Glp1r*$^{Wnt1+/+}$mice (Figures 4I and 4J). However, although semaglutide attenuated the sickness and hypothermia in cecal slurry-treated control mice, these actions of semaglutide were absent in *Glp1r*$^{Wnt1-/-}$ mice (Figures 4I and 4J). Blood and spleen bacterial loads were lower in semaglutide-treated control but not in *Glp1r*$^{Wnt1-/-}$ mice (Figure 4K), whereas semaglutide had no effect on liver and lung bacterial loads in either genotype (Figure S4E).

Examining parameters of systemic inflammation, in contrast to findings in wild-type control mice, semaglutide failed to attenuate levels of TNF-α, IL-1β, IL-6, and IL-10 in plasma and lung of cecal slurry-treated *Glp1r*$^{Wnt1-/-}$ mice (Figures 4L, 4M, S4F, and S4G). Semaglutide had no effect on plasma or lung CXCL1 or IFN-γ levels in either genotype (Figures S4F and S4G), although plasma IL-2 levels were higher in semaglutide-treated control but not *Glp1r*$^{Wnt1-/-}$ mice (Figure S4F). Concordant with the protein assays, semaglutide failed to downregulate lung *Tnf* and *Il1b* in *Glp1r*$^{Wnt1-/-}$ mice (Figure S4H). Lung *Il6* expression did not change in the semaglutide-treated group (Figure S4H). Semaglutide downregulated lung *Mmp9*, *Timp1*, and *Ly6g* expression in control mice but not in *Glp1r*$^{Wnt1-/-}$ mice (Figure 4N). Similarly, semaglutide-treated control mice had lower lung injury scores and numbers of lung elastase-positive neutrophils, effects that were abolished in *Glp1r*$^{Wnt1-/-}$ mice (Figures 4O and 4P). Collectively, semaglutide protects against polymicrobial sepsis-associated pathologies, including sickness behaviors, hypothermia, systemic inflammation, and lung injury, actions which require the expression of neuronal GLP-1Rs.

Blocking α_1-adrenergic signaling abolishes the anti-inflammatory effects of GLP-1RAs on LPS-induced inflammation

We next explored possible pathways through which GLP-1R activation attenuates TLR-mediated inflammation, using plasma TNF-α as a readout. Administration of GLP-1RAs can modify plasma lipid species involved in inflammation, including lipid mediators.[38] These lipid species may lower plasma cytokines, including TNF-α.[39] Accordingly, we performed lipidomics analyses on the plasma of C57BL/6J mice treated with LPS and exendin-4 i.p. and quantified the lipid mediators by targeted lipidomics and major classes of lipids by untargeted lipidomics. However, exendin-4 had no effect on the levels of plasma lipid species detected, including lipid mediators derived from arachidonic acid, eicosapentaenoic acid, and docosahexaenoic acid (Table S1), and lipids, including glycerolipids, phospholipids, sphingolipids, and sterols (Table S2). Hence, suppression of

(C–H) (C) The lung bacterial load, (D) plasma cytokine levels, (E) lung cytokine levels, (F) lung *Mmp9, Timp1*, and *Ly6g* expression, (G) lung injury scores from hematoxylin and eosin-stained sections, and (H) lung immunohistochemistry staining of neutrophil elastase in C57BL/6J mice 24 h after i.p. injection of vehicle or cecal slurry (600 μg/kg) and subcutaneous injection of vehicle or semaglutide (2.44 nmol/kg). For (F), expression was reported relative to *Tbp* (a reference gene). For (G), green arrows indicate neutrophil infiltration. Scale bars, 100 μm. n = 5–12. Data were pooled from two independent experiments.
(I and J) (I) Sepsis scores and (J) rectal temperature of *Glp1r*$^{Wnt1+/+}$ and *Glp1r*$^{Wnt1-/-}$ mice over 24 h after i.p. injection of cecal slurry (600 μg/kg) and subcutaneous injection of vehicle or semaglutide (2.44 nmol/kg). n = 9–14. Data were pooled from four independent experiments.
(K–P) (K) Blood and spleen bacterial loads, (L) plasma cytokine levels, (M) lung cytokine levels, (N) lung *Mmp9, Timp1*, and *Ly6g* expression, (O) lung injury scores from hematoxylin and eosin-stained sections, and (P) lung immunohistochemistry staining of neutrophil elastase in *Glp1r*$^{Wnt1+/+}$ and *Glp1r*$^{Wnt1-/-}$ mice 24 h after i.p. injection of cecal slurry (600 μg/kg) and subcutaneous injection of vehicle or semaglutide (2.44 nmol/kg). For (N), expression was reported relative to *Tbp* (a reference gene). For (O), green arrows indicate neutrophil infiltration. Scale bars, 100 μm. n = 8–14. Data were pooled from four independent experiments.
Data are represented as mean ± SD. *p < 0.05, **p < 0.01, *** p < 0.001, **** p < 0.0001. Two-way ANOVA tests with Sidak post hoc tests in (A)–(P). For (A) and (B), the asterisks denote the Sidak post hoc test comparisons between the cecal slurry + vehicle vs. cecal slurry + semaglutide groups. For (I) and (J), the asterisks denote the Sidak post hoc test comparisons between the *Glp1r*$^{Wnt1+/+}$ + vehicle vs. *Glp1r*$^{Wnt1+/+}$ + semaglutide groups.

Please cite this article in press as: Wong et al., Central glucagon-like peptide 1 receptor activation inhibits Toll-like receptor agonist-induced inflammation, Cell Metabolism (2023), https://doi.org/10.1016/j.cmet.2023.11.009

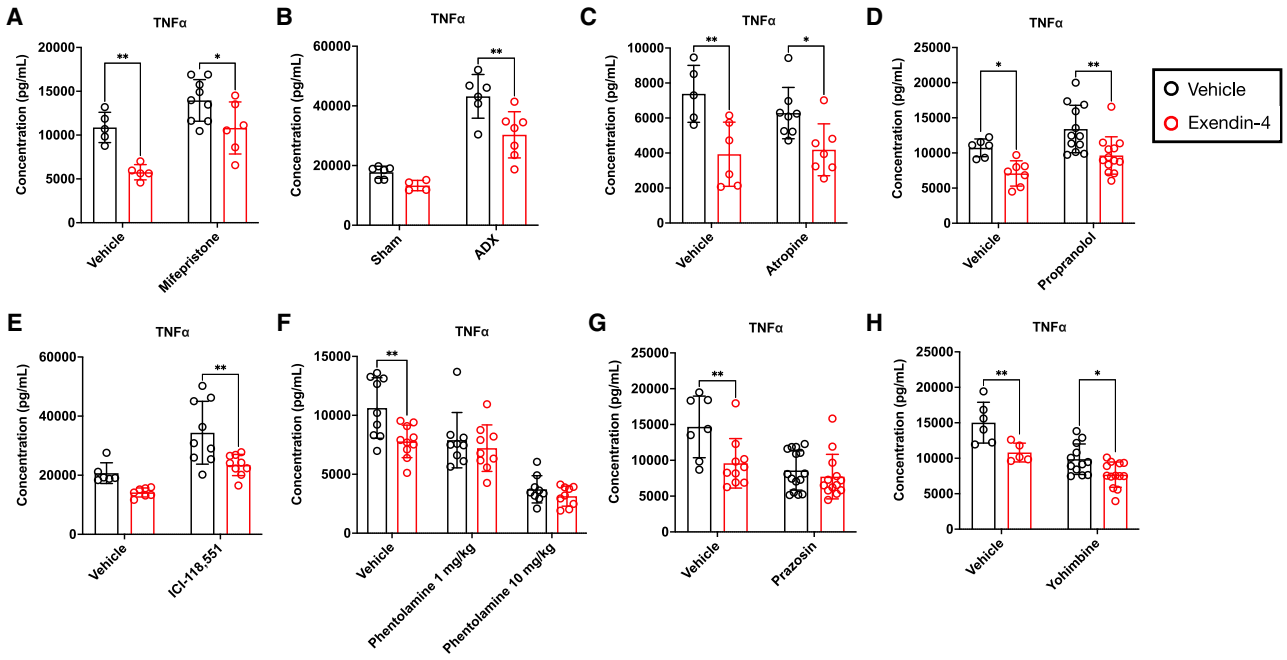

Figure 5. Antagonism of the α_1-adrenergic receptor abolishes the decrease in TNF-α levels following exendin-4 treatment

(A) Plasma TNF-α in C57BL/6J mice treated with mifepristone (10 mg/kg) i.p. for 1 h followed by LPS (35 μg) and exendin-4 (10 nmol/kg) or vehicle (saline) i.p. for 1 h. n = 5–9. Data were pooled from two independent experiments.

(B) Plasma TNF-α in sham or bilaterally adrenalectomized (ADX) C57BL/6J mice treated with LPS (35 μg) and exendin-4 (10 nmol/kg) or vehicle (saline) i.p. for 1 h. n = 4–7. Data were pooled from two independent experiments.

(C–H) Plasma TNF-α in C57BL/6J mice pre-treated i.p. with the following cholinergic and adrenergic inhibitors: (C) atropine (1 mg/kg) for 10 min, (D) propranolol (5 mg/kg) for 30 min, (E) ICI-118,551 (5 mg/kg) for 30 min, (F) phentolamine (1 or 10 mg/kg) for 15 min, (G) prazosin (1 mg/kg) for 15 min, and (H) yohimbine (1 mg/kg) for 15 min, followed by LPS (35 μg) and exendin-4 (10 nmol/kg) or vehicle (saline) i.p. for 1 h. n = 4–10 in vehicle groups, n = 6–15 in cholinergic and adrenergic inhibitor groups. Each panel comprises data pooled from two independent experiments.

Data are represented as mean ± SD. *p < 0.05, **p < 0.01. Two-way ANOVA tests with Sidak post hoc tests in (A)–(H).

LPS-induced inflammation by exendin-4 is not associated with changes in the plasma lipid species measured.

The CNS also regulates the peripheral immune system via the hypothalamic-pituitary-adrenal (HPA) axis and the autonomic nervous system (ANS).[18] We first explored the role of the HPA axis in mediating the effect of exendin-4 on TNF-α. In rodents, i.c.v. injection of GLP-1RAs raises plasma corticosterone levels by activation of the HPA axis,[40] which may result in peripheral immunosuppression. We used both pharmacological and surgical methods to address the putative role of the HPA axis. Treatment with mifepristone, an anti-glucocorticoid and anti-progestogen, enhanced LPS-induced TNF-α levels in C57BL/6J mice (Figure 5A). Yet, exendin-4 still prevented the full induction of TNF-α by LPS in mice treated with mifepristone (Figure 5A). We next studied adrenalectomized (ADX) mice, which had markedly lower plasma corticosterone levels than sham-operated mice (Figure S5A). LPS-treated ADX mice had higher TNF-α levels than LPS-treated sham-operated controls. However, TNF-α levels were lower in ADX mice in response to exendin-4 administration (Figure 5B). Collectively, the decrease in plasma TNF-α upon GLP-1R activation did not involve the HPA axis.

Within the ANS, the sympathetic nervous system suppresses peripheral immune responses by neuroendocrine activation of adrenergic receptors on lymphocytes, monocytes, and macrophages.[41,42] In the parasympathetic nervous system, vagal afferent nerves relay peripheral cytokine signals to the CNS, which then activates the HPA axis.[43,44] Vagal efferent nerves can inhibit TNF-α produced by splenic macrophages directly in an acetylcholine-dependent manner,[45,46] or indirectly via the splanchnic nerve in the sympathetic nervous system.[47] The increase in heart rate by GLP-1RAs via both the sympathetic and parasympathetic nervous systems represents a related example of ANS control via similar mechanisms.[48]

We pre-treated C57BL/6J mice with various inhibitors of ANS signaling, followed by administration of LPS and exendin-4. Atropine, an anticholinergic that inhibits parasympathetic tone, did not attenuate the inhibitory effect of exendin-4 on LPS-induced plasma TNF-α levels (Figure 5C). Nevertheless, the same dose of atropine, inhibited gastric emptying (Figure S5B). Hence, exendin-4 does not appear to act via cholinergic pathways to attenuate LPS-induced inflammation.

In the sympathetic nervous system, neuroendocrine release of adrenaline and noradrenaline leads to activation of α- and β-adrenergic receptors. Injection of the pan-β blocker propranolol augmented LPS-induced TNF-α levels but did not abrogate the effects of exendin-4 to reduce TNF-α levels (Figure 5D).[49] Nevertheless, the same dose of propranolol reduced basal heart rate in mice (Figure S5C). Among the subtypes of β-adrenergic receptors, the β_2-adrenergic receptor is abundantly expressed in macrophages and transduces anti-inflammatory actions.[50]

Please cite this article in press as: Wong et al., Central glucagon-like peptide 1 receptor activation inhibits Toll-like receptor agonist-induced inflammation, Cell Metabolism (2023), https://doi.org/10.1016/j.cmet.2023.11.009

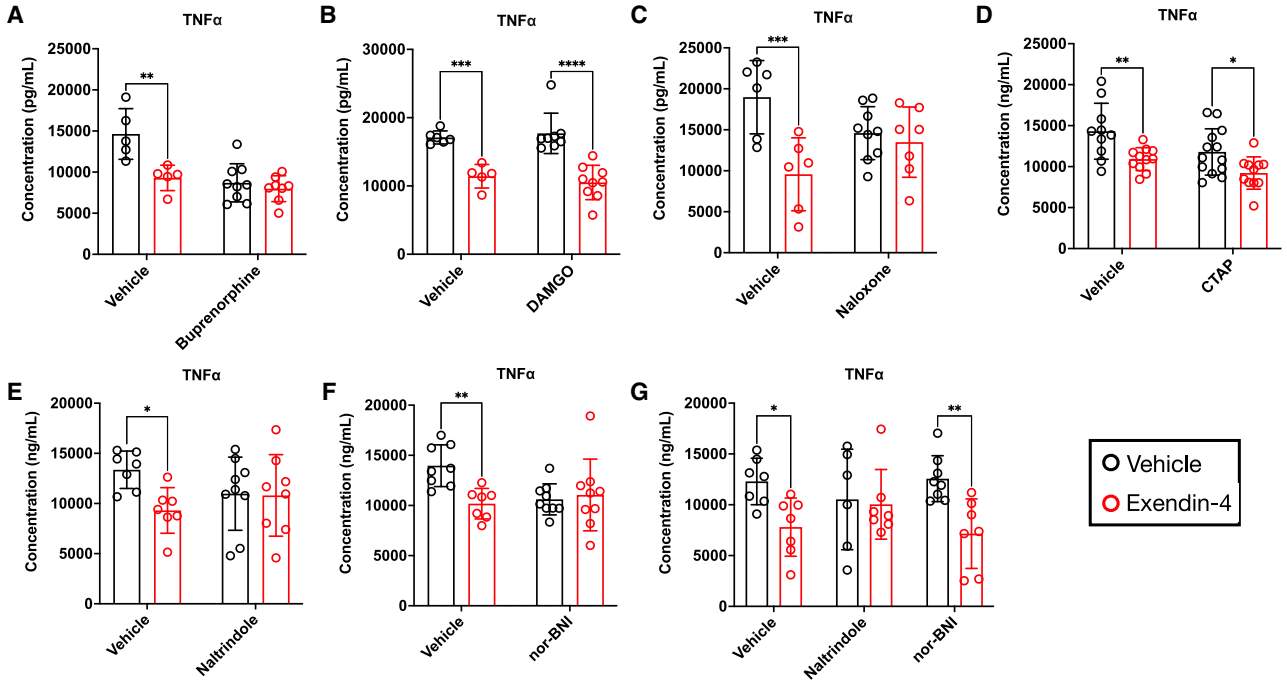

Figure 6. Antagonism of the δ- or κ-opioid receptor abolishes the decrease in TNF-α levels following exendin-4 treatment

(A–F) Plasma TNF-α levels in C57BL/6J mice pre-treated with the following opioid receptor agonists or antagonists: (A) buprenorphine (100 μg/kg) s.c. for 1 h, (B) DAMGO (1 mg/kg) i.p. for 15 min, (C) naloxone (1 mg/kg) i.p. for 15 min, (D) CTAP (1 mg/kg) i.p. for 15 min, (E) naltrindole (1 mg/kg) i.p. for 15 min, and (F) nor-BNI (1 mg/kg) i.p. for 15 min, followed by LPS (35 μg) and exendin-4 (10 nmol/kg) or vehicle (saline) i.p. for 1 h. n = 5–13. Each panel comprises data pooled from two independent experiments.

(G) Plasma TNF-α levels in C57BL/6J mice injected with naltrindole (1.5 μg), nor-BNI (1.5 μg), or vehicle (saline) i.c.v. for 30 min followed by LPS (35 μg) and exendin-4 (10 nmol/kg) or vehicle (saline) i.p. for 1 h. n = 6–8. Data were pooled from three independent experiments.

Data are represented as mean ± SD. *p < 0.05, **p < 0.01, ***p < 0.001, ****p < 0.0001. Two-way ANOVA tests with Sidak post hoc tests in (A)–(G).

β_2-adrenergic antagonism with ICI-118,551 enhanced plasma TNF-α levels in LPS-treated mice (Figure 5E).[51] However, consistent with the data for propranolol, ICI-118,551 had no effect on the anti-inflammatory actions of exendin-4 (Figure 5E).

We next assessed the consequence of α-adrenergic blockade. As opposed to β-blockers, the pan-α blocker phentolamine given at a dose of 10 mg/kg led to a decrease in TNF-α by LPS (Figure 5F),[52] and this dose of phentolamine abolished the inhibitory effects of exendin-4 on TNF-α (Figure 5F). At a dose of 1 mg/kg, phentolamine had a less pronounced effect on TNF-α yet still abolished the effects of exendin-4 on TNF-α (Figure 5F). This lower dose of phentolamine was sufficient to induce tachycardia in conscious mice (Figure S5C), a known effect of pan-α-adrenergic agonists.[53] To ascertain the α-adrenergic receptor subtypes involved in the anti-inflammatory effect of exendin-4, we pre-treated LPS-challenged mice with either prazosin, an α_1-adrenergic antagonist, or yohimbine, an α_2-adrenergic antagonist. Similar to findings with phentolamine, both prazosin and, to a lesser extent, yohimbine blunted the LPS-induced TNF-α response (Figures 5G and 5H).[49,54] In prazosin-treated mice, exendin-4 treatment did not lead to a decrease in plasma TNF-α (Figure 5G), but in yohimbine-treated mice, plasma TNF-α was lower in the exendin-4 vs. vehicle group (Figure 5H). Notably, prazosin did not affect the reduction in TNF-α by dexamethasone (Figure S5D), suggesting that blocking α_1-adrenergic receptors selectively abolished the anti-inflammatory effect of exendin-4.

Blocking δ- or κ-opioid receptors abolishes the anti-inflammatory effects of GLP-1RAs

In initial pilot experiments to test the effects of exendin(9-39) in the brain, we injected mice subcutaneously with the analgesic buprenorphine 1 h prior to the i.c.v. injections. However, exendin-4 had no effect on plasma TNF-α levels in LPS-treated mice given vehicle or exendin(9-39) i.c.v. (Figure S6A). We suspected that buprenorphine abolished the effect of exendin-4 on plasma TNF-α. In an independent set of experiments without i.c.v. injections, exendin-4 did not decrease plasma TNF-α in buprenorphine-treated mice challenged with LPS (Figure 6A). Consequently, we administered lidocaine topically as an analgesic in all of the i.c.v. experiments shown.

Buprenorphine is a partial agonist of the μ-opioid receptor and an antagonist of the δ- and κ-opioid receptors.[55] We postulated that the activation of the μ-opioid receptor and/or the inhibition of δ- and κ-opioid receptors (via buprenorphine) abolished the effect of exendin-4 on plasma TNF-α. Pre-treatment with the μ-opioid receptor agonist [D-Ala^2, *N*-MePhe^4, Gly-ol]-enkephalin (DAMGO) did not alter LPS-induced plasma TNF-α nor the inhibitory effect of exendin-4 (Figure 6B). DAMGO given at this dose effectively inhibited gastric emptying (Figure S6B), a known effect of opioid administration.[56] We next tested the effect of naloxone, an opioid antagonist that blocks μ-, δ-, and κ-opioid receptors. Naloxone itself had no effect on LPS-induced TNF-α, but it abolished the reduction of TNF-α in exendin-4-treated

Please cite this article in press as: Wong et al., Central glucagon-like peptide 1 receptor activation inhibits Toll-like receptor agonist-induced inflammation, Cell Metabolism (2023), https://doi.org/10.1016/j.cmet.2023.11.009

mice (Figure 6C). By contrast, naloxone did not abolish the lowering of TNF-α by dexamethasone (Figure S6C).

Next, we used specific antagonists to ascertain the opioid receptor subtypes that mediate the effect of exendin-4. Pre-treatment with the μ-opioid receptor-specific antagonist D-Phe-Cys-Tyr-D-Trp-Arg-Thr-Pen-Thr-NH_2 (CTAP) did not change plasma TNF-α in LPS-treated mice, nor did it abrogate the inhibitory effect of exendin-4 on TNF-α (Figure 6D). Naltrindole, a δ-opioid receptor-specific antagonist, also did not affect plasma TNF-α levels induced by LPS, but it eliminated the inhibitory effect of exendin-4 on TNF-α levels (Figure 6E). Similar to naltrindole, the κ-opioid receptor-specific antagonist norbinaltorphimine (nor-BNI) had no intrinsic effect on LPS-induced TNF-α but blocked the effect of exendin-4 on TNF-α levels (Figure 6F).

Although opioid receptors are mainly expressed centrally, these receptors are also expressed in the spinal cord and gut.[57] To localize the TNF-α-lowering effect of exendin-4 to the central δ- and/or κ-opioid receptor, we injected naltrindole or nor-BNI i.c.v. followed by an i.p. injection of LPS and exendin-4. Central administration of naltrindole, but not nor-BNI, abolished the inhibitory effect of exendin-4 on plasma TNF-α levels in LPS-treated mice (Figure 6G).

Lastly, we analyzed published single-nucleus RNA sequencing datasets, interrogating whether neural cells co-express *Glp1r*, *Adra1a*/*Adra1b*/*Adra1d* (encodes the three subtypes of α_1-adrenergic receptors), and *Oprd1* (encodes the δ-opioid receptor) in the hindbrain and/or hypothalamus. In the hindbrain dataset that spans the nucleus tractus solitarius and area postrema,[58] *Glp1r* was detected mainly in neurons rather than non-neuronal cells (Figure S6D). These neurons also expressed *Adra1a*, *Adra1b*, and *Oprd1* (Figure S6D). Similar to the hindbrain, *Glp1r* was expressed primarily in the neurons and minimally in non-neuronal cells in the hypothalamus (Figure S6E).[59] Based on the anatomical annotations,[59] neurons from the paraventricular nucleus of the hypothalamus, arcuate nucleus, and tuberal nucleus express high levels of *Glp1r* (Figure S6E). *Glp1r*$^+$ neurons in the paraventricular nucleus of the hypothalamus and tuberal nucleus express *Adra1a* but not *Adra1b* (Figure S6E). A cluster of *Glp1r*$^+$ neurons in the arcuate nucleus co-express *Adra1a*, *Adra1b*, and *Oprd1* (Figure S6E). *Adra1d* was not detected in any of these datasets. Importantly, *in situ* hybridization data from the Allen Brain Atlas revealed labeling of both *Glp1r* and *Oprd1* in the pontine gray of the hindbrain (Figure S6F).[60] By contrast, *Adra1a*/*Adra1d* were mainly detected in the medulla oblongata of the hindbrain (not shown), and no data on *Adra1b* were available from the atlas.

DISCUSSION

The innate immune system recognizes micro-organism components and the inflammatory responses that ensue, constituting the first line of defense against foreign pathogens, but dysfunction in the innate immune system response can lead to overt, uncontrolled inflammation resulting in various inflammatory disorders.[61] Here, we show that GLP-1RAs reduce inflammation caused by both synthetic (Pam3CSK4 and CpG) and natural, pathogen-derived (zymosan, LPS, flagellin, and live bacteria from cecal slurry) ligands of various TLRs. These data extend the anti-inflammatory actions of GLP-1RAs, first described for LPS, to other pro-inflammatory TLR agonists. GLP-1RA treatment led to reduced LPS-induced plasma TNF-α through mechanisms requiring neuronal GLP-1Rs, the α_1-adrenergic receptor, and the δ- and κ-opioid receptor. Our findings propose a common and central mechanism of GLP-1RAs against inflammation induced by activation of various TLRs. Given the low level of GLP-1R expression within circulating and tissue resident TLR-expressing immune cells, our new data indicate an important role of CNS GLP-1Rs to indirectly counteract peripheral TLR-mediated inflammation.

The concerted anti-inflammatory actions of GLP-1RAs on the gut T cell GLP-1R,[14,15] and on central neuronal GLP-1Rs as shown here, expands our mechanistic understanding of how GLP-1RAs reduce inflammation and tissue injury in diseases characterized by disordered and excess inflammation. GLP-1RAs dampen T cell-mediated inflammation directly by acting on the gut intraepithelial lymphocyte GLP-1R,[14] as opposed to TLR-induced inflammation, where the anti-inflammatory actions of GLP-1RAs are mediated centrally. Because both adrenergic and opioid signaling are immunosuppressive,[62,63] central GLP-1R activation appears to recruit these pathways to suppress inflammation. The type and origin of inflammation dictates whether peripheral and/or central GLP-1Rs are involved in the anti-inflammatory actions of GLP-1RAs.

Tirzepatide binds both the GLP-1R and GIPR,[64] with its weight loss effect mediated via the GLP-1R in mice,[65] likely via GLP-1Rs expressed in central neurons. By contrast, although the inhibitory effect of GLP-1RAs, including exendin-4 and semaglutide, on LPS-induced inflammation was abolished in *Glp1r*$^{Nes-/-}$ mice, tirzepatide still decreased plasma TNF-α in these mice lacking CNS GLP-1Rs. Because GIPR agonism can attenuate inflammation in adipose tissue, macrophages, and brain,[66,67] it seems likely that tirzepatide reduces inflammation via both the GLP-1R and the GIPR in mice with LPS-induced inflammation.

Cecal slurry injection induces polymicrobial sepsis by disseminating cecal bacteria into the peritoneum that subsequently reach peripheral organs, triggering overt inflammation and tissue injury. Semaglutide ameliorated the sickness behaviors, hypothermia, and systemic inflammation caused by the polymicrobial infection. Moreover, semaglutide protected against infection-associated lung injury by inhibiting local inflammation and preventing neutrophil infiltration, effects that were recently demonstrated in a cecal slurry- and hyperoxia-induced lung injury model using another GLP-1RA, liraglutide.[36] Here, we showed that GLP-1RAs require the expression of neuronal GLP-1Rs to mitigate polymicrobial sepsis, implying that GLP-1RAs attenuate sepsis-associated dysfunction through their central anti-inflammatory effects. GLP-1RAs did not consistently lower bacterial loads in multiple organs, implying that the attenuated inflammation unlikely resulted from the inhibition of bacterial infection. Notably, TNF-α is known to mediate sickness behaviors, hypothermia, and neutrophil extravasation during acute lung injury.[68–70] Taken together, GLP-1R activation, acting via central neuronal GLP-1Rs, attenuates multiple sepsis-associated pathologies resulting from the downstream actions of pro-inflammatory cytokines, particularly TNF-α.

Central GLP-1R activity also controls heart rate,[48,71] gastric emptying,[29] gastropancreatic exocrine secretion,[72] and food intake.[29] Although the specific brain regions mediating the peripheral anti-inflammatory effect of GLP-1RAs remain to be

precisely identified, candidate regions likely express high levels of GLP-1Rs and may be distinct from those that control metabolic functions. The GLP-1R in the dorsal vagal complex of the brainstem and hypothalamus mediates many physiological effects of GLP-1,[5] and expression of *Glp1r* in these parts of the brain was reduced in $Glp1r^{Wnt1-/-}$ mice.[29] *Glp1r*, *Adra1a*, and *Oprd1* were co-localized to specific regions of the hindbrain and the hypothalamus. Collectively, we suspect that GLP-1RAs suppress peripheral inflammation, likely by activating hindbrain and/or hypothalamic GLP-1Rs. As the central hub of autonomic signals, the dorsal vagal complex expresses all of the machinery necessary to regulate peripheral inflammation, including GLP-1,[73] catecholamines,[74] enkephalin,[75] and their cognate receptors, further bolstering the relevance of the dorsal vagal complex GLP-1R. Representing another potential site of action for GLP-1RAs to inhibit peripheral inflammation, the limbic system also expresses the GLP-1R,[76] and neuronal activity in the limbic system is controlled by the endogenous opioid system.[77]

Our studies of the inhibitory actions of GLP-1RAs on immune-cell-dependent inflammation provide an important framework for understanding the efficacy of GLP-1RAs on numerous seemingly unrelated diseases.[1,14] GLP-1RAs reduce rates of cardiovascular disease and are being tested in phase 3 trials of metabolic liver disease, kidney disease, and Alzheimer's disease, disorders known to be exacerbated by dysregulated immune responses.[1,5] Improvements in the acute TLR-mediated inflammation model conferred by GLP-1RAs do not require the metabolic benefits of GLP-1RAs, dissociating the anti-inflammatory properties of GLP-1RAs from reductions in glycemia or body weight. In addition, previous studies in murine models of diet-induced obesity, steatohepatitis, and atherosclerosis failed to link the anti-inflammatory actions of GLP-1RAs to the myeloid cell GLP-1R,[6–10,12] likely due to the low expression of the GLP-1R in myeloid cells.[8,13] Our current data extend the importance of the gut-CNS-GLP-1R axis to encompass the systemic control of TLR-dependent inflammation, actions with broad importance for understanding how GLP-1RAs constrain inflammation and reduce the chronic complications of metabolic disease.

Limitations of the study

Our studies demonstrated acute anti-inflammatory effects of exendin-4 on TLR-dependent inflammation, but whether the same mechanisms and pathways transduce chronic effects of GLP-1RAs to reduce inflammation, in mice with diabetes or obesity, has not been studied here. Models with chronic, low-grade inflammation involving myeloid cells where GLP-1RAs have shown therapeutic potential, such as diet-induced obesity, steatohepatitis, or atherosclerosis models may provide more insights. Although 1 μg of exendin(9-39) given i.c.v. did not result in detectable levels of exendin(9-39) in the blood, it did not preclude the possibility that a very small amount of exendin(9-39) enters the circulation and blocks peripheral GLP-1Rs. TNF-α was chosen as a key readout throughout our LPS studies, but other cytokines, such as IL-10, could also be involved in the anti-inflammatory actions of GLP-1RAs. The precise neuronal locations of the anti-inflammatory actions of GLP-1RAs in the brain remains to be identified, and non-neuronal cells in the brain such as astrocytes, oligodendrocytes, and pericytes that express the GLP-1R may also contribute to these actions.[5] It is not clear how blocking the α_1-adrenergic receptor and κ-opioid receptor signaling peripherally abolishes the effects of GLP-1RAs on LPS-induced TNF-α. Moreover, only male mice were studied here; hence, ongoing studies in male and female mice should refine the precise neuro-immune pathways linking CNS GLP-1Rs to suppression of peripheral inflammation.

STAR★METHODS

Detailed methods are provided in the online version of this paper and include the following:

- KEY RESOURCES TABLE
- RESOURCE AVAILABILITY
  - Lead contact
  - Materials availability
  - Data and code availability
- EXPERIMENTAL MODEL AND STUDY PARTICIPANT DETAILS
  - Animal studies
- METHOD DETAILS
  - Drug and chemical treatment
  - Analyte measurements
  - Gene expression analysis
  - Flow cytometry
  - Peritoneal lavage collection
  - Cytokine secretion assays
  - Intracerebroventricular injection
  - Cecal slurry model
  - Histology
  - Lipidomics
  - Gastric emptying
  - Heart rate measurement
  - Analyses of published single nucleus RNA sequencing datasets
  - Statistical analysis

SUPPLEMENTAL INFORMATION

Supplemental information can be found online at https://doi.org/10.1016/j.cmet.2023.11.009.

ACKNOWLEDGMENTS

We thank Louise Brown at the LTRI Microscopy Core, Toronto, Canada; Lois Kelsey at The Centre for Phenogenomic, Toronto, Canada; and Fatima Sultani at the Analytical Facility for Bioactive Molecules, The Hospital for Sick Children, Toronto, Canada for technical assistance on the slide scanning, heart rate measurement, and lipidomics experiments, respectively. We appreciate the critical discussions on this work with Professor Susan George Bahl at the University of Toronto, Toronto, Canada. These studies were funded by operating grants from the Canadian Institute for Health Research 154321 and Novo Nordisk Inc., all to D.J.D. C.K.W. was supported by a BBDC Sellers Postdoctoral Fellowship and BBDC D. H. Gales Family Charitable Foundation Postdoctoral Fellowship.

AUTHOR CONTRIBUTIONS

C.K.W., B.A.M., L.L.B., J.A.K., R.H., N.R., J.M.Y., and T.J.B. designed and executed the experiments and edited the manuscript. R.J.S. provided $Glp1r^{flox/flox}$ mice and edited the manuscript. D.J.D. designed the experiments and both C.K.W. and D.J.D. wrote the manuscript.

DECLARATION OF INTERESTS

D.J.D. has consulted for Altimmune, Amgen, Kallyope, Merck, Novo Nordisk, Pfizer Inc., and Sanofi Inc. Mt. Sinai Hospital receives operating grant support from Amgen, Novo Nordisk, and Pfizer Inc. for studies in the Drucker lab. R.J.S. has consulted for Novo Nordisk, Scohia, CinRx, Fractyl, Structure Therapeutics, Congruenc Therapeutics, Calibrate, and Rewind and receives operating grant support from Novo Nordisk, Astra Zeneca, Fractyl, and Eli Lilly Inc.

Received: March 20, 2023
Revised: October 16, 2023
Accepted: November 21, 2023
Published: December 18, 2023

REFERENCES

1. Drucker, D.J. (2018). Mechanisms of action and therapeutic application of glucagon-like Peptide-1. Cell Metab. *27*, 740–756.
2. Drucker, D.J. (2016). The cardiovascular biology of glucagon-like Peptide-1. Cell Metab. *24*, 15–30.
3. Yabut, J.M., and Drucker, D.J. (2023). Glucagon-like Peptide-1 receptor-based therapeutics for metabolic liver disease. Endocr. Rev. *44*, 14–32.
4. Kopp, K.O., Glotfelty, E.J., Li, Y., and Greig, N.H. (2022). Glucagon-like peptide-1 (GLP-1) receptor agonists and neuroinflammation: implications for neurodegenerative disease treatment. Pharmacol. Res. *186*, 106550.
5. McLean, B.A., Wong, C.K., Campbell, J.E., Hodson, D.J., Trapp, S., and Drucker, D.J. (2021). Revisiting the complexity of GLP-1 action from sites of synthesis to receptor activation. Endocr. Rev. *42*, 101–132.
6. Lee, Y.S., Park, M.S., Choung, J.S., Kim, S.S., Oh, H.H., Choi, C.S., Ha, S.Y., Kang, Y., Kim, Y., and Jun, H.S. (2012). Glucagon-like peptide-1 inhibits adipose tissue macrophage infiltration and inflammation in an obese mouse model of diabetes. Diabetologia *55*, 2456–2468.
7. Somm, E., Montandon, S.A., Loizides-Mangold, U., Gaïa, N., Lazarevic, V., De Vito, C., Perroud, E., Bochaton-Piallat, M.L., Dibner, C., Schrenzel, J., and Jornayvaz, F.R. (2021). The GLP-1R agonist liraglutide limits hepatic lipotoxicity and inflammatory response in mice fed a methionine-choline deficient diet. Transl. Res. *227*, 75–88.
8. McLean, B.A., Wong, C.K., Kaur, K.D., Seeley, R.J., and Drucker, D.J. (2021). Differential importance of endothelial and hematopoietic cell GLP-1Rs for cardiometabolic vs. hepatic actions of semaglutide. JCI Insight *6*, e153732.
9. Trevaskis, J.L., Griffin, P.S., Wittmer, C., Neuschwander-Tetri, B.A., Brunt, E.M., Dolman, C.S., Erickson, M.R., Napora, J., Parkes, D.G., and Roth, J.D. (2012). Glucagon-like peptide-1 receptor agonism improves metabolic, biochemical, and histopathological indices of nonalcoholic steatohepatitis in mice. Am. J. Physiol. Gastrointest. Liver Physiol. *302*, G762–G772.
10. Moschovaki Filippidou, F., Kirsch, A.H., Thelen, M., Kétszeri, M., Artinger, K., Aringer, I., Schabhüttl, C., Mooslechner, A.A., Frauscher, B., Pollheimer, M., et al. (2020). Glucagon-like Peptide-1 receptor agonism improves nephrotoxic serum nephritis by inhibiting T-cell proliferation. Am. J. Pathol. *190*, 400–411.
11. McLean, B.A., Wong, C.K., Kabir, M.G., and Drucker, D.J. (2022). Glucagon-like Peptide-1 receptor Tie2+ cells are essential for the cardioprotective actions of liraglutide in mice with experimental myocardial infarction. Mol. Metab. *66*, 101641.
12. Noyan-Ashraf, M.H., Shikatani, E.A., Schuiki, I., Mukovozov, I., Wu, J., Li, R.K., Volchuk, A., Robinson, L.A., Billia, F., Drucker, D.J., and Husain, M. (2013). A glucagon-like peptide-1 analog reverses the molecular pathology and cardiac dysfunction of a mouse model of obesity. Circulation *127*, 74–85.
13. Hadjiyanni, I., Siminovitch, K.A., Danska, J.S., and Drucker, D.J. (2010). Glucagon-like peptide-1 receptor signalling selectively regulates murine lymphocyte proliferation and maintenance of peripheral regulatory T cells. Diabetologia *53*, 730–740.
14. Wong, C.K., Yusta, B., Koehler, J.A., Baggio, L.L., McLean, B.A., Matthews, D., Seeley, R.J., and Drucker, D.J. (2022). Divergent roles for the gut intraepithelial lymphocyte GLP-1R in control of metabolism, microbiota, and T cell-induced inflammation. Cell Metab. *34*, 1514–1531.e7.
15. Yusta, B., Baggio, L.L., Koehler, J., Holland, D., Cao, X., Pinnell, L.J., Johnson-Henry, K.C., Yeung, W., Surette, M.G., Bang, K.W., et al. (2015). GLP-1R agonists modulate enteric immune responses through the intestinal intraepithelial lymphocyte GLP-1R. Diabetes *64*, 2537–2549.
16. Lu, Y.C., Yeh, W.C., and Ohashi, P.S. (2008). LPS/TLR4 signal transduction pathway. Cytokine *42*, 145–151.
17. Akira, S., and Takeda, K. (2004). Toll-like receptor signalling. Nat. Rev. Immunol. *4*, 499–511.
18. Sternberg, E.M. (2006). Neural regulation of innate immunity: a coordinated nonspecific host response to pathogens. Nat. Rev. Immunol. *6*, 318–328.
19. Lebrun, L.J., Lenaerts, K., Kiers, D., Pais de Barros, J.P., Le Guern, N., Plesnik, J., Thomas, C., Bourgeois, T., Dejong, C.H.C., Kox, M., et al. (2017). Enteroendocrine L Cells Sense LPS after gut barrier injury to enhance GLP-1 secretion. Cell Rep. *21*, 1160–1168.
20. Rakipovski, G., Rolin, B., Nøhr, J., Klewe, I., Frederiksen, K.S., Augustin, R., Hecksher-Sørensen, J., Ingvorsen, C., Polex-Wolf, J., and Knudsen, L.B. (2018). The GLP-1 analogs liraglutide and semaglutide reduce atherosclerosis in ApoE(-/-) and LDLr(-/-) mice by a mechanism that includes inflammatory pathways. JACC Basic Transl. Sci. *3*, 844–857.
21. Chaudhuri, A., Ghanim, H., Vora, M., Sia, C.L., Korzeniewski, K., Dhindsa, S., Makdissi, A., and Dandona, P. (2012). Exenatide exerts a potent antiinflammatory effect. J. Clin. Endocrinol. Metab. *97*, 198–207.
22. Rodbard, H.W., Rosenstock, J., Canani, L.H., Deerochanawong, C., Gumprecht, J., Lindberg, S.Ø., Lingvay, I., Søndergaard, A.L., Treppendahl, M.B., and Montanya, E.; Investigators; P. (2019). Oral semaglutide versus empagliflozin in patients with Type 2 diabetes uncontrolled on metformin: the Pioneer 2 trial. Diabetes Care *42*, 2272–2281.
23. Michalek, S.M., Moore, R.N., McGhee, J.R., Rosenstreich, D.L., and Mergenhagen, S.E. (1980). The primary role of lymphoreticular cells in the mediation of host responses to bacterial endotoxim. J. Infect. Dis. *141*, 55–63.
24. Grivennikov, S.I., Tumanov, A.V., Liepinsh, D.J., Kruglov, A.A., Marakusha, B.I., Shakhov, A.N., Murakami, T., Drutskaya, L.N., Förster, I., Clausen, B.E., et al. (2005). Distinct and nonredundant in vivo functions of TNF produced by T cells and macrophages/neutrophils: protective and deleterious effects. Immunity *22*, 93–104.
25. Fonseca, M.T., Moretti, E.H., Marques, L.M.M., Machado, B.F., Brito, C.F., Guedes, J.T., Komegae, E.N., Vieira, T.S., Festuccia, W.T., Lopes, N.P., and Steiner, A.A. (2021). A leukotriene-dependent spleen-liver axis drives TNF production in systemic inflammation. Sci. Signal. *14*, eabb0969.
26. Marino, M.W., Dunn, A., Grail, D., Inglese, M., Noguchi, Y., Richards, E., Jungbluth, A., Wada, H., Moore, M., Williamson, B., et al. (1997). Characterization of tumor necrosis factor-deficient mice. Proc. Natl. Acad. Sci. USA *94*, 8093–8098.
27. Zhao, K., Kirman, I., Tschepen, I., Schwab, R., and Weksler, M.E. (1997). Peritoneal lavage reduces lipopolysaccharide-induced elevation of serum TNF-alpha and IL-6 mortality in mice. Inflammation *21*, 379–390.
28. Cork, S.C., Richards, J.E., Holt, M.K., Gribble, F.M., Reimann, F., and Trapp, S. (2015). Distribution and characterisation of Glucagon-like peptide-1 receptor expressing cells in the mouse brain. Mol. Metab. *4*, 718–731.
29. Varin, E.M., Mulvihill, E.E., Baggio, L.L., Koehler, J.A., Cao, X., Seeley, R.J., and Drucker, D.J. (2019). Distinct Neural Sites of GLP-1R Expression Mediate Physiological versus Pharmacological Control of incretin Action. Cell Rep. *27*, 3371–3384.e3.
30. Sundman, E., and Olofsson, P.S. (2014). Neural control of the immune system. Adv. Physiol. Educ. *38*, 135–139.

31. Sisley, S., Gutierrez-Aguilar, R., Scott, M., D'Alessio, D.A., Sandoval, D.A., and Seeley, R.J. (2014). Neuronal GLP1R mediates liraglutide's anorectic but not glucose-lowering effect. J. Clin. Invest. *124*, 2456–2463.

32. Baggio, L.L., and Drucker, D.J. (2021). Glucagon-like peptide-1 receptor co-agonists for treating metabolic disease. Mol. Metab. *46*, 101090.

33. Lewis, A.J., Seymour, C.W., and Rosengart, M.R. (2016). Current murine models of sepsis. Surg. Infect. (Larchmt) *17*, 385–393.

34. Costa, E.L., Schettino, I.A., and Schettino, G.P. (2006). The lung in sepsis: guilty or innocent? Endocr. Metab. Immune Disord. Drug Targets *6*, 213–216.

35. Sato, T., Shimizu, T., Fujita, H., Imai, Y., Drucker, D.J., Seino, Y., and Yamada, Y. (2020). GLP-1 receptor signaling differentially modifies the outcomes of sterile vs viral pulmonary inflammation in male mice. Endocrinology *161*, bqaa201.

36. Baer, B., Putz, N.D., Riedmann, K., Gonski, S., Lin, J., Ware, L.B., Toki, S., Peebles, R.S., Jr., Cahill, K.N., and Bastarache, J.A. (2023). Liraglutide pretreatment attenuates sepsis-induced acute lung injury. Am. J. Physiol. Lung Cell. Mol. Physiol. *325*, L368–L384.

37. Kawabata, K., Hagio, T., and Matsuoka, S. (2002). The role of neutrophil elastase in acute lung injury. Eur. J. Pharmacol. *451*, 1–10.

38. Zobel, E.H., Wretlind, A., Ripa, R.S., Rotbain Curovic, V., von Scholten, B.J., Suvitaival, T., Hansen, T.W., Kjær, A., Legido-Quigley, C., and Rossing, P. (2021). Ceramides and phospholipids are downregulated with liraglutide treatment: results from the LiraFlame randomized controlled trial. BMJ Open Diabetes Res. Care *9*, e002395.

39. Serhan, C.N., Chiang, N., Dalli, J., and Levy, B.D. (2014). Lipid mediators in the resolution of inflammation. Cold Spring Harb. Perspect. Biol. *7*, a016311.

40. Larsen, P.J., Tang-Christensen, M., and Jessop, D.S. (1997). Central administration of glucagon-like peptide-1 activates hypothalamic neuroendocrine neurons in the rat. Endocrinology *138*, 4445–4455.

41. Rosas-Ballina, M., Olofsson, P.S., Ochani, M., Valdés-Ferrer, S.I., Levine, Y.A., Reardon, C., Tusche, M.W., Pavlov, V.A., Andersson, U., Chavan, S., et al. (2011). Acetylcholine-synthesizing T cells relay neural signals in a vagus nerve circuit. Science *334*, 98–101.

42. Körner, A., Schlegel, M., Kaussen, T., Gudernatsch, V., Hansmann, G., Schumacher, T., Giera, M., and Mirakaj, V. (2019). Sympathetic nervous system controls resolution of inflammation via regulation of repulsive guidance molecule A. Nat. Commun. *10*, 633.

43. Watkins, L.R., Goehler, L.E., Relton, J.K., Tartaglia, N., Silbert, L., Martin, D., and Maier, S.F. (1995). Blockade of interleukin-1 induced hyperthermia by subdiaphragmatic vagotomy: evidence for vagal mediation of immune-brain communication. Neurosci. Lett. *183*, 27–31.

44. Steinberg, B.E., Silverman, H.A., Robbiati, S., Gunasekaran, M.K., Tsaava, T., Battinelli, E., Stiegler, A., Bouton, C.E., Chavan, S.S., Tracey, K.J., and Huerta, P.T. (2016). Cytokine-specific neurograms in the sensory vagus nerve. Bioelectron. Med. *3*, 7–17.

45. Borovikova, L.V., Ivanova, S., Zhang, M., Yang, H., Botchkina, G.I., Watkins, L.R., Wang, H., Abumrad, N., Eaton, J.W., and Tracey, K.J. (2000). Vagus nerve stimulation attenuates the systemic inflammatory response to endotoxin. Nature *405*, 458–462.

46. Wang, H., Yu, M., Ochani, M., Amella, C.A., Tanovic, M., Susarla, S., Li, J.H., Wang, H., Yang, H., Ulloa, L., et al. (2003). Nicotinic acetylcholine receptor alpha7 subunit is an essential regulator of inflammation. Nature *421*, 384–388.

47. Martelli, D., Yao, S.T., McKinley, M.J., and McAllen, R.M. (2014). Reflex control of inflammation by sympathetic nerves, not the vagus. J. Physiol. *592*, 1677–1686.

48. Baggio, L.L., Ussher, J.R., McLean, B.A., Cao, X., Kabir, M.G., Mulvihill, E.E., Mighiu, A.S., Zhang, H., Ludwig, A., Seeley, R.J., et al. (2017). The autonomic nervous system and cardiac GLP-1 receptors control heart rate in mice. Mol. Metab. *6*, 1339–1349.

49. Elenkov, I.J., Haskó, G., Kovács, K.J., and Vizi, E.S. (1995). Modulation of lipopolysaccharide-induced tumor necrosis factor-alpha production by selective alpha- and beta-adrenergic drugs in mice. J. Neuroimmunol. *61*, 123–131.

50. Tan, K.S., Nackley, A.G., Satterfield, K., Maixner, W., Diatchenko, L., and Flood, P.M. (2007). Beta2 adrenergic receptor activation stimulates pro-inflammatory cytokine production in macrophages via PKA- and NF-kappaB-independent mechanisms. Cell. Signal. *19*, 251–260.

51. Verhoeckx, K.C., Doornbos, R.P., van der Greef, J., Witkamp, R.F., and Rodenburg, R.J. (2005). Inhibitory effects of the beta-adrenergic receptor agonist zilpaterol on the LPS-induced production of TNF-alpha in vitro and in vivo. J. Vet. Pharmacol. Ther. *28*, 531–537.

52. Mastronardi, C.A., Yu, W.H., and McCann, S. (2001). Lipopolysaccharide-induced tumor necrosis factor-alpha release is controlled by the central nervous system. Neuroimmunomodulation *9*, 148–156.

53. Morpurgo, C., Faini, D., and Falcone, A. (1975). Effects of phentolamine, dihydroergocristine and isoxsuprine on the blood pressure and heart rate in normotensive, hypotensive and hypertensive rats. Naunyn Schmiedebergs Arch. Pharmacol. *290*, 335–346.

54. Staedtke, V., Bai, R.Y., Kim, K., Darvas, M., Davila, M.L., Riggins, G.J., Rothman, P.B., Papadopoulos, N., Kinzler, K.W., Vogelstein, B., et al. (2018). Disruption of a self-amplifying catecholamine loop reduces cytokine release syndrome. Nature *564*, 273–277.

55. Lutfy, K., and Cowan, A. (2004). Buprenorphine: a unique drug with complex pharmacology. Curr. Neuropharmacol. *2*, 395–402.

56. De Luca, A., and Coupar, I.M. (1996). Insights into opioid action in the intestinal tract. Pharmacol. Ther. *69*, 103–115.

57. Stein, C. (2016). Opioid receptors. Annu. Rev. Med. *67*, 433–451.

58. Dowsett, G.K.C., Lam, B.Y.H., Tadross, J.A., Cimino, I., Rimmington, D., Coll, A.P., Polex-Wolf, J., Knudsen, L.B., Pyke, C., and Yeo, G.S.H. (2021). A survey of the mouse hindbrain in the fed and fasted states using single-nucleus RNA sequencing. Mol. Metab. *53*, 101240.

59. Steuernagel, L., Lam, B.Y.H., Klemm, P., Dowsett, G.K.C., Bauder, C.A., Tadross, J.A., Hitschfeld, T.S., Del Rio Martin, A., Chen, W., de Solis, A.J., et al. (2022). HypoMap-a unified single-cell gene expression atlas of the murine hypothalamus. Nat. Metab. *4*, 1402–1419.

60. Lein, E.S., Hawrylycz, M.J., Ao, N., Ayres, M., Bensinger, A., Bernard, A., Boe, A.F., Boguski, M.S., Brockway, K.S., Byrnes, E.J., et al. (2007). Genome-wide atlas of gene expression in the adult mouse brain. Nature *445*, 168–176.

61. Shaw, A.C., Goldstein, D.R., and Montgomery, R.R. (2013). Age-dependent dysregulation of innate immunity. Nat. Rev. Immunol. *13*, 875–887.

62. Chhatar, S., and Lal, G. (2021). Role of adrenergic receptor signalling in neuroimmune communication. Curr. Res Immunol. *2*, 202–217.

63. Plein, L.M., and Rittner, H.L. (2018). Opioids and the immune system - friend or foe. Br. J. Pharmacol. *175*, 2717–2725.

64. Hammoud, R., and Drucker, D.J. (2023). Beyond the pancreas: contrasting cardiometabolic actions of GIP and GLP1. Nat. Rev. Endocrinol. *19*, 201–216.

65. Samms, R.J., Christe, M.E., Collins, K.A., Pirro, V., Droz, B.A., Holland, A.K., Friedrich, J.L., Wojnicki, S., Konkol, D.L., Cosgrove, R., et al. (2021). GIPR agonism mediates weight-independent insulin sensitization by tirzepatide in obese mice. J. Clin. Invest. *131*, e146353.

66. Zhang, Z.Q., and Hölscher, C. (2020). GIP has neuroprotective effects in Alzheimer and Parkinson's disease models. Peptides *125*, 170184.

67. Mantelmacher, F.D., Zvibel, I., Cohen, K., Epshtein, A., Pasmanik-Chor, M., Vogl, T., Kuperman, Y., Weiss, S., Drucker, D.J., Varol, C., et al. (2019). GIP regulates inflammation and body weight by restraining myeloid-cell-derived S100A8/A9. Nat. Metab. *1*, 58–69.

68. Dantzer, R., O'Connor, J.C., Freund, G.G., Johnson, R.W., and Kelley, K.W. (2008). From inflammation to sickness and depression: when the immune system subjugates the brain. Nat. Rev. Neurosci. *9*, 46–56.

69. Leon, L.R., White, A.A., and Kluger, M.J. (1998). Role of IL-6 and TNF in thermoregulation and survival during sepsis in mice. Am. J. Physiol. *275*, R269–R277.

70. Jones, M.R., Simms, B.T., Lupa, M.M., Kogan, M.S., and Mizgerd, J.P. (2005). Lung NF-kappaB activation and neutrophil recruitment require IL-1 and TNF receptor signaling during pneumococcal pneumonia. J. Immunol. *175*, 7530–7535.

71. Holt, M.K., Cook, D.R., Brierley, D.I., Richards, J.E., Reimann, F., Gourine, A.V., Marina, N., and Trapp, S. (2020). PPG neurons in the nucleus of the solitary tract modulate heart rate but do not mediate GLP-1 receptor agonist-induced tachycardia in mice. Mol. Metab. *39*, 101024.

72. Wettergren, A., Wøjdemann, M., and Holst, J.J. (1998). Glucagon-like peptide-1 inhibits gastropancreatic function by inhibiting central parasympathetic outflow. Am. J. Physiol. *275*, G984–G992.

73. Larsen, P.J., Tang-Christensen, M., Holst, J.J., and Orskov, C. (1997). Distribution of glucagon-like peptide-1 and other preproglucagon-derived peptides in the rat hypothalamus and brainstem. Neuroscience *77*, 257–270.

74. Levitt, P., and Moore, R.Y. (1979). Origin and organization of brainstem catecholamine innervation in the rat. J. Comp. Neurol. *186*, 505–528.

75. Mansour, A., Hoversten, M.T., Taylor, L.P., Watson, S.J., and Akil, H. (1995). The cloned mu, delta and kappa receptors and their endogenous ligands: evidence for two opioid peptide recognition cores. Brain Res. *700*, 89–98.

76. Jensen, C.B., Pyke, C., Rasch, M.G., Dahl, A.B., Knudsen, L.B., and Secher, A. (2018). Characterization of the glucagonlike Peptide-1 receptor in male mouse brain using a novel antibody and in situ hybridization. Endocrinology *159*, 665–675.

77. Le Merrer, J., Becker, J.A., Befort, K., and Kieffer, B.L. (2009). Reward processing by the opioid system in the brain. Physiol. Rev. *89*, 1379–1412.

78. Hao, Y., Hao, S., Andersen-Nissen, E., Mauck, W.M., 3rd, Zheng, S., Butler, A., Lee, M.J., Wilk, A.J., Darby, C., Zager, M., et al. (2021). Integrated analysis of multimodal single-cell data. Cell *184*, 3573–3587.e29.

79. Starr, M.E., Steele, A.M., Saito, M., Hacker, B.J., Evers, B.M., and Saito, H. (2014). A new cecal slurry preparation protocol with improved long-term reproducibility for animal models of sepsis. PLoS One *9*, e115705.

80. Baggio, L.L., Huang, Q., Brown, T.J., and Drucker, D.J. (2004). Oxyntomodulin and glucagon-like peptide-1 differentially regulate murine food intake and energy expenditure. Gastroenterology *127*, 546–558.

81. Shrum, B., Anantha, R.V., Xu, S.X., Donnelly, M., Haeryfar, S.M., McCormick, J.K., and Mele, T. (2014). A robust scoring system to evaluate sepsis severity in an animal model. BMC Res. Notes *7*, 233.

82. Matute-Bello, G., Downey, G., Moore, B.B., Groshong, S.D., Matthay, M.A., Slutsky, A.S., and Kuebler, W.M.; Acute Lung Injury in Animals Study Group (2011). An official American Thoracic Society workshop report: features and measurements of experimental acute lung injury in animals. Am. J. Respir. Cell Mol. Biol. *44*, 725–738.

83. Aprikian, O., Reynaud, D., Pace-Asciak, C., Leone, P., Blancher, F., Monnard, I., Darimont, C., and Macé, K. (2007). Neonatal dietary supplementation of arachidonic acid increases prostaglandin levels in adipose tissue but does not promote fat mass development in guinea pigs. Am. J. Physiol. Regul. Integr. Comp. Physiol. *293*, R2006–R2012.

84. Schenkel, L.C., Singh, R.K., Michel, V., Zeisel, S.H., da Costa, K.A., Johnson, A.R., Mudd, H.S., and Bakovic, M. (2015). Mechanism of choline deficiency and membrane alteration in postural orthostatic tachycardia syndrome primary skin fibroblasts. FASEB J. *29*, 1663–1675.

85. Chu, V., Otero, J.M., Lopez, O., Morgan, J.P., Amende, I., and Hampton, T.G. (2001). Method for non-invasively recording electrocardiograms in conscious mice. BMC Physiol. *1*, 6.

Please cite this article in press as: Wong et al., Central glucagon-like peptide 1 receptor activation inhibits Toll-like receptor agonist-induced inflammation, Cell Metabolism (2023), https://doi.org/10.1016/j.cmet.2023.11.009

STAR★METHODS

KEY RESOURCES TABLE

REAGENT or RESOURCE	SOURCE	IDENTIFIER
Antibodies		
Rat Anti-CD16/CD32 Antibody	BioLegend	CAT: 101301 RRID: AB_312800
Alexa Fluor 488 Anti-F4/80 Antibody	BioLegend	CAT: 100425 RRID: AB_493520
PE Anti-Ly6C Antibody	BioLegend	CAT: 128008 RRID: AB_1186132
PE/Cyanine7 Anti-CD45.2 Antibody	BioLegend	CAT: 109830 RRID: AB_1186098
APC Anti-B220 Antibody	BioLegend	CAT: 103212 RRID: AB_312997
APC/Cyanine7 Anti-CD11b Antibody	BioLegend	CAT: 101226 RRID: AB_830642
Pacific Blue Anti-Ly6G Antibody	BioLegend	CAT: 127612 RRID: AB_2251161
Brilliant Violet 510 Anti-CD3 Antibody	BioLegend	CAT: 100234 RRID: AB_2562555
Neutrophil Elastase (E8U3X) Rabbit mAb	Cell Signalling Technology	CAT: 90120 RRID: N/A
Chemicals, peptides, and recombinant proteins		
Exendin-4	Chi Scientific	Custom synthesis
Lipopolysaccharides (LPS) from *Escherichia coli* O111:B4	MilliporeSigma	CAT: L2630-10MG
Pam3CSK4	Invivogen	CAT: tlrl-pms
Poly (I:C) HMW	Invivogen	CAT: tlrl-pic-5
Ultrapure flagellin from S. typhimurium	Invivogen	CAT: tlrl-epstfla-5
R848	Invivogen	CAT: tlrl-r848-5
CpG ODN 1826	Invivogen	CAT: tlrl-1826-1
Dexamethasone	MilliporeSigma	CAT: D1756
Dexamethasone-21 phosphate	MilliporeSigma	CAT: D1159
Semaglutide	Novo Nordisk	N/A
Tirzepatide	Eli Lilly	N/A
Exendin(9-39)	Chi Scientific	Custom synthesis
Mifepristone	MilliporeSigma	CAT: M8046
Atropine sulfate monohydrate	Fisher Scientific	CAT: AAA1023609
Propranolol hydrochloride	MilliporeSigma	CAT: P0884
ICI 118,551 hydrochloride	MilliporeSigma	CAT: I127
Phentolamine hydrochloride	MilliporeSigma	CAT: P7547
Prazosin hydrochloride	MilliporeSigma	CAT: P7791
Yohimbine hydrochloride	MilliporeSigma	CAT: Y3125
Buprenorphine	Ceva	N/A
Lidocaine	Aspen	CAT: 021
[D-Ala^2, N-Me-Phe^4, Gly^5-ol]-Enkephalin (DAMGO) acetate salt	MilliporeSigma	CAT: E7384
Naloxone hydrochloride dihydrate	MilliporeSigma	CAT: N7758
CTAP	MilliporeSigma	CAT: C6352
Naltrindole hydrochloride	MilliporeSigma	CAT: N115

(*Continued on next page*)

Please cite this article in press as: Wong et al., Central glucagon-like peptide 1 receptor activation inhibits Toll-like receptor agonist-induced inflammation, Cell Metabolism (2023), https://doi.org/10.1016/j.cmet.2023.11.009

Continued

REAGENT or RESOURCE	SOURCE	IDENTIFIER
Nor-Binaltorphimine (nor-BNI) dihydrochloride	Calbiochem	CAT: 5.08017.0001
Acetaminophen	MilliporeSigma	CAT: A7085
RBC lysis buffer	BioLegend	CAT: 420301
RPMI 1640	Wisent Bioproducts	CAT: 350-000-EL
Fetal bovine serum	Wisent Bioproducts	CAT: 080-150
Penicillin-Streptomycin, 100x	Thermo Fisher	CAT: 15140148
SYTOX AADvanced dead cell stain kit (SYTOX-AAD)	Thermo Fisher	CAT: S10349
SuperScript III Reverse Transcriptase	Thermo Fisher	CAT: 18080085
TaqMan Fast Advanced Master Mix	Thermo Fisher	CAT: 4444965
Trypticase-Soy-Agar plates	Wissent Bioproducts	Custom order
SignalStain Boost IHC Detection Reagent (HRP, Rabbit)	Cell Signalling Technology	CAT: 8114
ImmPACT DAB Substrate Kit, Peroxidase	Vector Laboratories	CAT: SK-4105
Critical commercial assays		
V-PLEX Proinflammatory Panel 1 Mouse Kit	Mesoscale	CAT: K15048D
V-PLEX Mouse TNF-α Kit	Mesoscale	CAT: K152QWD
V-PLEX Mouse MCP-1 Kit	Mesoscale	CAT: K152NND
Mouse / Rat Corticosterone ELISA	ALPCO	CAT: 55-CORMS-E01
Exendin-4 (Heloderma suspectum) - EIA Kit	Phoenix Pharmaceuticals	CAT: EK-070-94
Acetaminophen L3K assays	Sekisui	CAT: 506-10
Experimental models: Organisms/strains		
Mouse: C57BL/6J	Jackson Laboratory	CAT: 000664 RRID: IMSR_JAX:000664
Mouse: B6.Cg-Tg(Tek-cre)1Ywa/J	Jackson Laboratory	CAT: 008863 RRID: IMSR_JAX:008863
Mouse: B6.Cg-Tg(Nes-cre)1Kln/J	Jackson Laboratory	CAT: 003771 RRID: IMSR_JAX:003771
Mouse: B6.Cg-*E2f1*$^{Tg(Wnt1\text{-}cre)2Sor}$/J	Jackson Laboratory	CAT: 022501 RRID: IMSR_JAX:022501
Mouse: *Glp1r*$^{fl/fl}$	Randy Seeley	N/A
Oligonucleotides		
Tnf Taqman assays	Thermo Fisher	Mm00443258_m1
Adam17 Taqman assays	Thermo Fisher	Mm00456428_m1
Adgre1 Taqman assays	Thermo Fisher	Mm00802529_m1
Ccl2 Taqman assays	Thermo Fisher	Mm00441242_m1
Ccl4 Taqman assays	Thermo Fisher	Mm00443111_m1
Ccr2 Taqman assays	Thermo Fisher	Mm01216173_m1
Il1b Taqman assays	Thermo Fisher	Mm00434228_m1
Il6 Taqman assays	Thermo Fisher	Mm00446190_m1
Tlr4 Taqman assays	Thermo Fisher	Mm00445273_m1
Glp1r Taqman assays	Thermo Fisher	Mm00445292_m1
Mmp9 Taqman assays	Thermo Fisher	Mm00442991_m1
Timp Taqman assays	Thermo Fisher	Mm00441818_m1
Ly6g Taqman assays	Thermo Fisher	Mm04934123_m1
Software and algorithms		
R 4.1.1	https://www.r-project.org/	N/A
Rstudio 1.4.1717	https://www.rstudio.com/	RRID: SCR_000432
Seurat 4.2.0	Hao et al.[78]	RRID: SCR_007322

(*Continued on next page*)

Please cite this article in press as: Wong et al., Central glucagon-like peptide 1 receptor activation inhibits Toll-like receptor agonist-induced inflammation, Cell Metabolism (2023), https://doi.org/10.1016/j.cmet.2023.11.009

Continued

REAGENT or RESOURCE	SOURCE	IDENTIFIER
GraphPad Prism 9	GraphPad	RRID: SCR_002798
Kaluza 2.1	Beckman Coulter	RRID: SCR_016182
QuPATH 0.44	Starr et al.[79]	RRID: SCR_018257
Other		
Teklad global 18% protein rodent diets (regular chow)	Envigo	CAT: 2018

RESOURCE AVAILABILITY

Lead contact

Daniel J Drucker (drucker@lunenfeld.ca) is the lead contact and takes full responsibility for the data in this paper. Further information and requests for resources and reagents should be directed to and will be fulfilled by the lead contact.

Materials availability

No unique reagents or materials were generated in these studies.

Data and code availability

No proprietary data or code is associated with this manuscript. All unprocessed data used for plotting the figures and supplemental information in the manuscript are available as Data S1. Any additional information required to reanalyze the data reported in this paper is available from the lead contact upon request.

EXPERIMENTAL MODEL AND STUDY PARTICIPANT DETAILS

Animal studies

All animal protocols were approved by the Animal Care and Use Subcommittee at the Toronto Centre for Phenogenomics at Mount Sinai Hospital (Toronto, Canada). Male mice (females were not studied) were housed as groups of up to five per cage in holding rooms with lights on between 7 am to 7 pm and ad libitum access to water and a chow diet (Enivgo).

Ten to twelve-week-old male C57BL/6J mice were obtained from Jackson Laboratory. *Glp1r*$^{fl/fl}$ mice were provided by Randy Seeley.[31] *Glp1r*$^{Tie2-/-}$,[8] *Glp1r*$^{Wnt1-/-}$,[29] and *Glp1r*$^{Nes-/-}$ mice,[31] were generated by crossing Tie2-Cre, Wnt1-Cre2, and Nestin-Cre mice with *Glp1r*$^{fl/fl}$ mice respectively. *Glp1r*$^{Tie2+/+}$, *Glp1r*$^{Wnt1+/+}$, and *Glp1r*$^{Nes+/+}$ mice represented control animals pooled from Cre-positive controls (Tie2-Cre;Glp1r$^{+/+}$, Wnt1-Cre2;Glp1r$^{+/+}$, and Nestin-Cre;*Glp1r*$^{+/+}$ respectively) and Cre-negative floxed controls (*Glp1r*$^{fl/fl}$). Male mice produced from these crossings were used in all TLR agonist and cecal slurry experiments. All male Cre-positive controls and *Glp1r*$^{fl/fl}$ mice show similar responses of exendin-4 to LPS-induced TNF-α.

Male C57BL/6J mice that had undergone bilateral adrenalectomy or sham surgery were purchased from Jackson Laboratory. The surgery was performed on mice six-seven weeks old, and the operated mice were allowed to recover for at least three weeks before the LPS experiments. Both sham and adrenalectomized mice were maintained on 0.9% saline instead of water after the surgery.

METHOD DETAILS

Drug and chemical treatment

For all *in vivo* TLR agonist experiments, exendin-4 (10 nmol/kg) (Chi Scientific) and various TLR agonists were injected i.p.. One to three hours after the injections, the mice were euthanized, and their tissues were collected for RNA and protein analyses. All TLR agonist-exendin-4 experiments were performed on mice that had no prior exposure to exogenous TLR agonists.

For LPS-semaglutide experiments, mice naïve to LPS were injected with semaglutide (2.44 nmol/kg; or 10 μg/kg) subcutaneously for one hour, followed by i.p. injection with LPS for one hour. For LPS-tirzepatide experiments, the mice used in the LPS-semaglutide experiments were allowed to recover for four weeks. The tirzepatide treatments for these mice were crossed over, i.e. the vehicle group in the LPS-semaglutide experiments received tirzepatide, and the semaglutide group received vehicle. These mice were injected subcutaneously with tirzepatide for one hour, followed by i.p. injection with LPS for one hour.

The following TLR agonists were used in this study: Pam3CSK4 (Invivogen), zymosan (Invivogen), polyinosinic:polycytidylic acid (poly I:C; Invivogen), LPS O111:B4 (MilliporeSigma), flagellin from *Salmonella typhimurium* (Invivogen), R848 (Invivogen), and CpG ODN 1826 (Invivogen). The following drugs were used in this study: exendin-4 (Chi Scientific), semaglutide (Novo Nordisk), tirzepatide (Eli Lily), dexamethasone (MilliporeSigma), and dexamethasone 21-phosphate (MilliporeSigma). The following antagonists were given prior to LPS treatment: exendin(9-39) (Chi Scientific), mifepristone (MilliporeSigma), atropine (MilliporeSigma), propranolol (MilliporeSigma), ICI-118,551 (MilliporeSigma), phentolamine (MilliporeSigma), prazosin (MilliporeSigma), yohimbine (MilliporeSigma), buprenorphine (Ceva), DAMGO (MilliporeSigma), naloxone (MilliporeSigma), CTAP (MilliporeSigma), naltrindole

Please cite this article in press as: Wong et al., Central glucagon-like peptide 1 receptor activation inhibits Toll-like receptor agonist-induced inflammation, Cell Metabolism (2023), https://doi.org/10.1016/j.cmet.2023.11.009

(MilliporeSigma), and nor-BNI (MilliporeSigma). For *in vitro* LPS experiments, dexamethasone dissolved in 0.1% (v/v) ethanol was used. For *in vivo* LPS experiments, the water-soluble dexamethasone 21-phosphate was used instead.

Analyte measurements

Blood was collected by saphenous vein or cardiac puncture into a tube coated with heparin lithium (Sarstedt) and supplemented with 1/10 TED (5000 KIU/mL Trasylol, 4 mM EDTA, 0.1 nM diprotin A). For plasma, blood samples were spun at 13000 g at 4°C for 5 minutes to recover the supernatant. Protein lysates were prepared by homogenizing tissues in a lysis buffer (50 mM Tris pH 8, 1 mM EDTA, 10% glycerol, 0.067% Brij-35) supplemented with protease inhibitors (MilliporeSigma) using the TissueLyzer II (Qiagen). ELISAs for TNF-α, IL-10, IL-12 p70, IL-1β, IL-6, CXCL1, IFNγ, IL-2, IL-4, IL-5, and MCP-1 (Meso Scale Discovery) were measured per manufacturer's instructions. For exendin(9-39) measurement, an exendin-4 ELISA (Phoenix Pharmaceuticals) that cross-reacts completely with the C-terminus of exendin(9-39) and exendin-4 was used. Its specificity for exendin(9-39) was confirmed with a standard curve prepared from exendin(9-39) (Chi Scientific) stock solution, which showed identical concentrations as the standard curve of equimolar exendin-4 (Figure S3D). Plasma corticosterone was measured with a corticosterone ELISA (ALPCO) per manufacturer's instructions.

Gene expression analysis

Blood leukocytes were prepared by lysing whole blood in an RBC lysis buffer (BioLegend) for 15 minutes. Lysed blood was washed with PBS, spun at 670 g for 3 minutes, and the recovered leukocytes were lysed in TRIzol. Peripheral tissues were homogenized in TRIzol using the TissueLyzer II. Total RNA was extracted with a standard chloroform and ethanol extraction protocol, followed by cDNA synthesis using SuperScript III (ThermoFisher) and analysis by quantitative PCR using Taqman assays (ThermoFisher). Relative expression was calculated using the $2^{-\Delta\Delta CT}$ method with *Tbp* as the reference gene (14706621, REF).

Flow cytometry

Cells were blocked with anti-CD16/CD32 (BioLegend) and stained with the following primary antibodies: CD45, CD3, CD19, CD11b, Ly6C, and Ly6G (BioLegend). SYTOX-AAD (ThermoFisher) was used as a viability stain. Stained samples were analyzed on the Gallios flow cytometer (Beckman Coulter).

Peritoneal lavage collection

To collect peritoneal lavage, a volume of 5 mL cold 0.5 mM EDTA in PBS was injected into the peritoneum of a euthanized mouse. The peritoneum was gently massaged to facilitate the release of the peritoneal cells. The lavage was withdrawn with a needle and a syringe and spun at 670 g for 3 minutes to recover the supernatant for TNF-α measurement and the cell pellet for flow cytometry.

Cytokine secretion assays

Whole blood culture was set up by mixing 100 μL freshly drawn mouse blood with 400 μL complete RPMI (RPMI1640, 10% FBS, 100 U/mL penicillin/streptomycin; ThermoFisher) per well in a 24-well plate. For culturing splenocytes, the spleen was mashed through a 40 μm cell strainer followed by an RBC lysis step, and 1 x 10^6 splenocytes resuspended in 500 μL complete RPMI were counted and seeded into each well of a 24-well plate. Whole blood or splenocyte culture was treated with 10 ng/mL LPS and vehicle, exendin-4, or dexamethasone for 6 hours. Culture supernatant was recovered at the end of the experiment for TNF-α measurement.

Intracerebroventricular injection

Intracerebroventricular (i.c.v.) injection was performed as described.[80] In the initial studies, mice were given buprenorphine (100 μg/kg) subcutaneously 30 minutes before the i.c.v. injection as a pre-emptive analgesic. When it was found that buprenorphine interfered with the effect of exendin-4 on TNF-α (Figure S6A), a 50 μL of 0.5% lidocaine (Aspen) was injected subcutaneously along the incision line on the scalp as a topical analgesic instead. For the i.c.v. procedures, mice were anaesthetized with isoflurane after which their scalp was incised. A Hamilton syringe with a 30-gauge needle was inserted into the lateral ventricle, and a volume of 5 μL of vehicle or antagonists loaded into the syringe was injected slowly. After the injection, the scalp was sutured, and the mice were allowed to rest for 30 minutes prior to LPS and exendin-4 injections.

Cecal slurry model

Cecal slurry was prepared from 10-week-old male C57BL/6J mice as described.[79] Cecal content was collected, resuspended in 15% glycerol, and serially passed through a 500-μm nylon mesh and a 70-μm cell strainer. The slurry was then aliquoted and cryopreserved at -80°C.

Male C57BL/6J *Glp1r*$^{Wnt1+/+}$ or *Glp1r*$^{Wnt1-/-}$ mice aged between 14 – 20 weeks old were injected i.p. with either vehicle (15% glycerol in saline) or 600 μg/kg cecal slurry and subcutaneously with vehicle (saline) or 2.44 nmol/kg semaglutide at the same time. At 3, 6, 9, and 24 hours after the injection, the core temperature of the mice were measured using a RET-3 mouse rectal probe (Braintree Scientific), and their sepsis phenotypes were scored as described.[81] The mice were euthanized 24 hours after the injection. Bacterial counts were quantified as colony forming units by spread plating 50 μL of whole blood or tissue lysates on trypticase soy agar plates (Wissent Bioproduct) incubated at 37°C for 24 hours, followed by counting of the colonies grown on the plates.

Histology

To prepare mouse lungs for histology in euthanized mice, the right bronchus was clamped with a haemostat, and 3 mL of 10% formalin was administered via the trachea to inflate the left lung at a rate of 200 μL/second. The inflated left lung was collected and further fixed in 10% formalin for 24 hours, followed by standard dehydration and paraffin embedding. Sections were subjected to hematoxylin and eosin staining for lung injury scoring, or immunohistochemistry for neutrophil elastase. Staining of neutrophil elastase was performed using a standard immunohistochemical staining protocol. Briefly, antigen retrieval was performed in a Tris-EDTA pH 9.0 antigen retrieval buffer at 95°C for 20 minutes using a decloaking chamber (Biocare Medical), followed by blocking, incubation with a rabbit anti-neutrophil elastase antibody (1/400; Cell Signalling Technology) at 4°C overnight, incubation with SignalStain Boost IHC Detection Reagent (Cell Signalling Technology) at room temperature for 30 minutes, and development of signals using ImmPACT DAB Substrate Kit, Peroxidase (Vector Laboratories). All slides were scanned at 20x using a Nanozoomer slide scanner (Hamamatsu). All image analyses were performed using QuPath 0.44. For lung injury scoring, ten high-power fields were generated randomly from each scanned section and scored in a blind manner as described previously based on the following five criteria: presence of neutrophils in alveolar space, presence of neutrophils in interstitial space, presence of hyaline membrane, proteinaceous debris in alveolar space, and septal thickening.[82] For elastase-positive neutrophil counts, ten high-power fields were generated randomly from each scanned section and counted manually in a blind manner.

Lipidomics

Targeted and untargeted lipidomics were performed on plasma samples from C57BL/6J mice treated with LPS and vehicle or exendin-4 for 1 hour. The liquid chromatography and tandem mass spectrometry experiments with the associated data analyses were performed by the Analytical Facility for Bioactive Molecules at the Hospital for Sick Children (Toronto, Canada) as previously described.[83,84] For targeted lipidomics experiments, samples spiked with internal standards were hydrolyzed in 10% KOH in methanol, evaporated under N_2 gas, reconstituted in 20%/80% water/acetonitrile, and ran on the Agilent 1290 uHPLC with a Sciex QTrap 5500. Lipid mediator concentrations were calculated by normalizing the peak area ratios of samples to the peak area ratios of extracted standard mixes of known concentration. For untargeted lipidomics experiments, samples spiked with internal standards underwent lipid extraction using chloroform. The chloroform layer recovered was evaporated under N_2 gas, reconstituted in acidified 2:1 methanol/chloroform, and ran by infusion MS/MS^{All} on a Sciex 6600 Q-TOF in both positive and negative ESI modes. Peak intensities were reported without normalization in Table S2.

Gastric emptying

Mice were fasted overnight from 5 pm to 9 am (17 hours) prior to the gastric emptying test. Fasted mice were treated with vehicle, atropine (MilliporeSigma), or DAMGO (MilliporeSigma) 15 minutes before a gavage of acetaminophen (100 mg/kg; MilliporeSigma). Blood was drawn from the tail vein at 15, 30, and 60 minutes after gavage and plasma was collected. Plasma acetaminophen levels were measured using an acetaminophen L3K assay (Sekisui).

Heart rate measurement

The heart rate in conscious mice was measured using the ECGenie system (MouseSpecfics).[85] The mouse was placed on the measurement platform to acclimatize for two minutes, and its echocardiogram (ECG) was recorded for two to five minutes. The ECG was analyzed on LabChart software (ADInstruments) and the heart rate was averaged from three sections of ECG tracings of 0.5-3 seconds each.

Analyses of published single nucleus RNA sequencing datasets

Published single nucleus RNA sequencing datasets on the brainstem NTS/AP (GSE166648)[58] and the hypothalamus (GSE208355)[59] were analyzed in Seurat 4.2,[78] as described previously.[14] The brainstem dataset was subjected to SCTransform, dimensional reduction, clustering, and UMAP plotting. The R object of the aggregated hypothalamus dataset containing all the processing steps was used directly for UMAP plotting.[59]

Statistical analysis

All data were presented as mean ± SD. Student's t test, one-way ANOVA, or two-way ANOVA were used where appropriate to calculate statistical significance. For two-way ANOVA, the statistical significance for comparisons between the GLP-1RA and vehicle group in the presence or absence of an intervention, including genotypes or treatments, was tested using the Sidak method as post-hoc tests to correct for multiple comparisons. Holm-Sidak tests were used to correct for multiple testing in lipidomics analyses.